JOURNAL OF CATALYSIS **109**, 433–462 (1988)

Events Observed and Evidence for Crystallite Migration in Pt/Al_2O_3 Catalysts

I. SUSHUMNA AND E. RUCKENSTEIN

Department of Chemical Engineering, State University of New York at Buffalo, Buffalo, New York 14260

Received February 3, 1987; revised July 28, 1987

The sintering behavior of model Pt/Al_2O_3 catalysts when heated in hydrogen, and alternately in H_2 and O_2 was investigated at different temperatures (between 300 and 800°C) by means of transmission electron microscopy. At both relatively low (500°C) and high temperatures (750°C), short-distance migration (usually 1–3 particle diameters) and coalescence of particles was observed to contribute considerably toward sintering. At 500°C and following two or three cycles of alternate heating in H_2 and O_2, significant migration of particles (up to 8-nm particles migrating over 25 nm) were observed on exposure of the oxidized particles to H_2 and/or of the reduced particles to O_2. Sintering is fast and pronounced in the initial 4 to 6 h of heating of a fresh sample; then it becomes slow. However, further continuous heating for extended periods of 12 h or more causes additional significant sintering by particle migration and coalescence among other mechanisms. This suggests that investigations based on only 1 or 2 h of heating, as often reported in the literature, yield incomplete information. The present results indicate that at both 500 and 750°C, sintering by ripening (apparently only of a localized kind) also occurs. The present results are evidence of the occurrence of a variety of phenomena such as short-distance migration and coalescence of particles, migration toward or away from another particle, decrease in size and/or disappearance of larger particles near unaffected smaller particles, decrease in size and/or disappearance of both small and larger particles, decrease in size and/or disappearance of small particles near larger particles (ripening), decrease in size and subsequent migration of particles or vice versa, collision without coalescence, and collision–coalescence–separation into two particles again. The particles seem to feel the presence of other nearby particles via long-range interparticle forces that induce the migration of a particle toward another or emission of atoms toward a nearby particle. The two major mechanisms of sintering of supported metal crystallites appear to be (i) short-distance, direction-selective (in contrast to random) migration of particles followed by (a) collision and coalescence or (b) direct transfer of atoms between the two approaching particles, or (ii) localized ripening (direct ripening) between a few stationary, adjacent particles.

INTRODUCTION

Alumina-supported Pt catalysts are relatively thermostable in comparison to supported Ag, Fe, Ni, etc. Nevertheless, Pt/Al_2O_3 catalysts still lose their activity gradually on use in reducing atmospheres (such as in catalytic reforming). A part of the activity loss is attributed to the sintering of the metal particles (*1–3*). The supported catalysts lose exposed surface area also during heating in oxidizing atmospheres (such as in automotive exhaust oxidation and during coke burn off) (*1, 4*). That is, coarsening of the supported crystallites occurs in both reducing and oxidizing atmospheres, though its extent may vary, depending on the catalyst system and the treatment conditions employed. In specific cases, such as Pt/Al_2O_3 heated in O_2 between 500 and 580°C, redispersion of the catalysts has also been observed (*5–10*). Basically, two physical models have frequently been employed to explain the growth kinetics of the supported crystallites (*11*). One, known as the crystallite migration model, considers that the growth occurs via random migration, collision, and coalescence of crystallites (*12, 13*). The other, known as the atomic migration

0021-9517/88 $3.00

model or Ostwald ripening, assumes that the growth occurs via emission of single atoms or molecules by the small crystallites and their capture by the larger crystallites (*14–16*). For single-atom emission and capture, two possibilities have been noted. In one of them, which is global, the small crystallites lose atoms to a surface phase of single atoms dispersed over the substrate, while the large ones capture atoms from this phase. In the other case, called direct ripening (*17*), atoms released by a small particle move directly to a neighboring large crystallite.

A number of investigations with supported catalysts including Pt/Al_2O_3 have been carried out in an attempt to identify the mechanisms involved in, and the factors responsible for, the growth of the crystallites, as well as for the regeneration of the sintered catalysts (*3, 11, 18–41*). Both model and industrial-type catalysts have been investigated, predominantly by selective chemisorption of gases, transmission electron microscopy, and X-ray line broadening (for reviews, see Refs. (*11, 14, 42–44*)). As a result of the anomalous chemisorption behavior (such as the suppression of room-temperature H_2 chemisorption following high-temperature (500°C) H_2 treatment) exhibited by certain catalyst systems such as Pt/Al_2O_3 (*45, 46*) and Pt/TiO_2 (*47–49*), it is now recognized that chemisorption of gases may require the availability of adsorption sites on the crystallites (which may be covered and hence prevent chemisorption, even though the dispersion is high). Consequently, there is not necessarily a direct correlation between the extent of chemisorption and the catalyst dispersion. Caution is needed therefore in drawing conclusions on the basis of dispersion values obtained from chemisorption measurements alone (*50*). A number of investigations of the mechanism of sintering of supported metal catalysts have relied on such chemisorption measurements. Selective chemisorption of gases is, in general, indeed a very valuable method of measuring catalyst dispersion. However, especially in cases where ambiguities and anomalies of the kind mentioned above are involved, it is appropriate to use a complementary technique such as electron microscopy. As is well known, transmission electron microscopy (TEM), though tedious, provides direct information on the crystallite shape, size, size distribution, and, to a large extent, on the mechanisms involved in sintering and redispersion. Therefore, TEM has been employed by a number of researchers to investigate the mechanism of sintering of supported metal catalysts.

The results have been discussed in terms of both Ostwald ripening (*8, 11, 14–18, 26–30, 37*) and crystallite migration models (*32–40*). On the basis of their electron microscopy or chemisorption results, a few authors (*26, 28, 29*) reported that they had never observed crystallite migration or dumbbell-shaped particles on the supports with the catalysts they had investigated and that atomic or molecular migration is the only mechanism of sintering and redispersion. Recent results, from this laboratory as well as from others, of direct TEM observation of changes in the same region of the samples following successive heat treatments have shown, however, that crystallites can migrate and that crystallite migration and coalescence contribute significantly to the growth of supported crystallites. Besides the early electron microscopy observations of supported crystallite migration by Bassett (*51*) in the case of copper and silver islands on carbon, graphite, or molybdenite substrates and by Skofronick *et al.* (*52*) in the case of gold islands on carbon and silicon substrates, there are more recent observations of supported crystallite migration and coalescence. Chu and Ruckenstein (*24*) observed significant migration of crystallites larger than 20 nm in the case of Pt/C heated in O_2 atmospheres. They observed migration of particles larger than 10 nm also in the case of Pt/Al_2O_3 at 750°C (*25*). Heinemann and Poppa (*53*) presented direct *in situ* electron microscopic evidence for the simultaneous occurrence of short-distance crystallite migration and coalescence as well as ripening in the sintering of Ag/graphite system in the temperature range 25–450°C. They noted that though slow ripening occurred over the entire temperature range, the overriding surface transport mechanism was short-distance (<10 nm) cluster mobility. Chen and Ruckenstein (*36*) in the case of Pd/Al_2O_3, Ruckenstein and Lee (*40*) in the case of Ni/Al_2O_3, and Sushumna and Ruckenstein (*39*) in the case of Fe/Al_2O_3 observed crystallite migration among a large number of other events when the samples were heated in H_2 and O_2. Arai *et al.* (*37*) reported *in situ* TEM results of sintering of Ni, Pt, and Ag on amorphous carbon, SiO_2, and Al_2O_3 and noted that in the case of Pt/Al_2O_3 and above 600°C, only particles larger than 10 nm grew through abrupt surface movement and subsequent coalescence of adjacent pairs. Richardson and Crump (*32*) in the case of Ni/SiO_2 concluded, on the basis of magnetic measurements of the particle size distributions, that especially above 450°C particle migration and coalescence were responsible for the sintering in a He atmosphere. Granquist and Buhrman (*54, 55*), analyzing various previous experimental results on sintering, argued on the basis of the shape of the particle size distributions that crystallite (migration and) coalescence is more likely than ripening to be responsible for the coarsening of the supported particles. Abundance of experimental results notwithstanding, the mechanism(s) of sintering has yet to be clarified; in general, some authors support one mechanism, while others support the other mechanism. However, recent results (*36, 39*) seem to suggest that the phenomena of sintering and regeneration involve complex interrelated processes that cannot be restricted to one or even to both of the mechanisms noted above.

In the past, investigations of supported metal catalysts, including Pt/Al_2O_3 have been based in general on either short (1 or 2 h) (*26–30, 41*) or long (24 or 48 h) durations of heating (*9, 25, 29*). However, no systematic investigations of short intervals of heating, especially of a fresh catalyst, over extended time periods, at various temperatures, have been carried out. Especially on the basis of 1 or 2 h of heating, a few authors have reported that they never observed crystallite migration on the supports with the catalysts they had investigated (*26–30*). Evidence for migration and coalescence with Pd/Al_2O_3 (*36*), Pt/Al_2O_3 (*25*), Ni/Al_2O_3 (*40*), and especially Fe/Al_2O_3 (*39*) have been presented from this laboratory among others in the past. Here we present additional transmission electron microscopic evidence for crystallite migration among other phenomena in Pt/Al_2O_3 model catalysts heated at different temperatures in H_2 and O_2.

EXPERIMENTAL

Preparation of Alumina Supports

The method of preparation of electron-transparent films of γ-Al_2O_3 has been described in detail previously (*25, 39*). Thin aluminum foils (99.999% pure, Alfa Products, Inc.) were cleaned thoroughly by chemical polishing and were subsequently washed in distilled water. An amorphous aluminum oxide layer about 30 nm thick was built up on the cleaned aluminum foil by anodic oxidation at 20 V in a 3 wt% tartaric acid solution. The oxidized foil was subsequently cleaned thoroughly in distilled water. The oxide layer was separated from aluminum by floating small pieces of the oxidized foil in mercuric chloride solution, in which the unoxidized aluminum dissolved. The aluminum oxide films were subsequently washed repeatedly in distilled water and eventually picked up on gold electron microscope grids. The oxide films on the grids were dried and subsequently heated at 800°C in laboratory air for about 72 h and then slowly cooled to the room temperature. The prolonged heat treatment is carried out to convert the amorphous films to crystalline γ-Al_2O_3 and to ensure that no further changes would occur on subsequent heat treatments. It is to be noted that after the above heat treatment and prior to or after the deposition of the metal, these alumina samples were not brought into contact with any solution or liquid and therefore no artifacts of the kind discussed by Glassl *et al.* (56) were likely to have been generated.

Platinum films 0.75, 1.5, and 2 nm thick were deposited onto the alumina films in three different batches, by evaporating the corresponding amounts of Pt wire (99.999% pure, Alfa Products, Inc.) from a tungsten filament in an Edwards vacuum evaporator. The vacuum in the chamber was better than 10^{-6} Torr. The substrate was maintained at room temperature during deposition.

It should be pointed out that the industrial supported Pt catalysts are relatively thermostable. The very low metal loading of Pt/Al_2O_3 usually used in industry contributes to the slow growth rate. The model catalysts in general have a relatively high loading, which enhances sintering. However, even though the metal loadings of the model catalysts may not correspond to those of the industrial catalysts, the model systems provide at least a qualitative indication of the processes that occur in supported catalyst systems. In this regard it is worth noting that Smith *et al.* (*41*) and Baker *et al.* (*27*) have noted previously that the behaviors of the model catalysts of the kind described here are in general similar to those of the industrial catalysts.

The samples on which metal had been deposited were heated in a quartz boat inside a quartz tube. Ultrapure hydrogen, both as-received (99.999% pure with <1 ppm O_2 and <3 ppm moisture) and further purified by being passed through a Deoxo unit (Engelhard Industries) followed by a column of 3-Å molecular sieves immersed in liquid nitrogen, were used in the experiments. Helium, 99.999% pure with <3 ppm moisture, was also passed through the above column of molecular sieves immersed in liquid nitrogen. Ultrahigh-purity-grade oxygen was used as received. All the gases were supplied by Linde Division, Union Carbide Corporation. For each heat treatment, the following procedure was adopted. With the sample inside, the tube was flushed with He for at least 5 minutes before the power to the furnace was turned on. The sample was heated in He until the preset temperature was reached, at which point He was turned off and the desired gas was let in. The sample was then heated for the predetermined length of time, at the end of which the furnace and the gas were turned off and He was allowed to flow through again. The sample was cooled slowly to the room temperature in He before it was exposed to the atmosphere.

The samples were observed in a JEOL 100U transmission electron microscope operated at 80 kV. Each sample was scanned thoroughly over the entire specimen area to check for uniformity in behavior, and pictures were taken at a few regions. Following each heat treatment, the same regions were photographed at the same magnification (in the 60–100-K range). Electron diffraction patterns were also recorded following each heat treatment. A liquid nitrogen trap was used to reduce specimen contamination in the microscope. Also, the intensity of the electron beam and the specimen's exposure to the beam were kept low to minimize the contamination of the specimen. The alumina film moved very little on the supporting grid, and, especially following the initial one or two observations, the same regions could be located relatively easily after successive heat treatments. The particle migrations shown in the next section were followed with reference to certain fixed grain boundaries or other "landmarks" on the support.

RESULTS

Table 1 lists some of the events observed on Pt/Al_2O_3 model catalysts heated in H_2 and O_2. Figures 1, 1′, and 1″ show some micrographs of the time sequence of a sam-

TABLE 1

Events Observed on Pt/Al$_2$O$_3$ Model Catalysts Heated in H$_2$ and O$_2$

Type	Event	Schematics	Figure Nos.
A	Migration, without coalescence, of small or large particles toward or away from another particle		1, 1′, 2, 2′, 3″, 5, 5
B	Migration, collision, and coalescence; gradual migration and coalescence		1, 1′, 1″, 2, 2′, 3″, 5, 5′, 6
C	Coalescence of nearby particles		1, 1′, 1″, 2, 3′, 3″
D	Migration followed by a decrease in size or vice versa		4, 5
E	Dumbbell-shaped particles, particles in fusion		1, 1′, 2, 2′, 3, 3″, 4
F	Coalescence of nearby larger particles adjacent to unaffected/decreasing smaller particles		1, 1′, 3″, 4
G	Transfer of atoms between two nearby particles via a neck or narrow whiskerlike bridge; formation and breakup of a contact between two particles via a narrow whiskerlike bridge		1, 1′, 3″
H	Decrease and/or disappearance of a small particle near a larger particle that grows in size or appears unaffected (ripening); decrease in size and/or disappearance of one particle amid particles of equal size		1, 1′, 4
I	Decrease of a large particle nearby smaller particles		4, 5, 5′
J	Disappearance of large and small particles	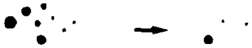	4, 5, 5′
K	Growth of smaller particles or coalescence of small particles to yield larger particles		1, 1′, 1″, 5, 5′
L	Collision, coalescence, and subsequent separation of two particles; separation of particles in contact		1, 1, 2, 6
M	Appearance of two particles in place of one (splitting, or wetting and reconstruction)	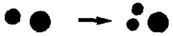	6
N	Overlapping particles		6

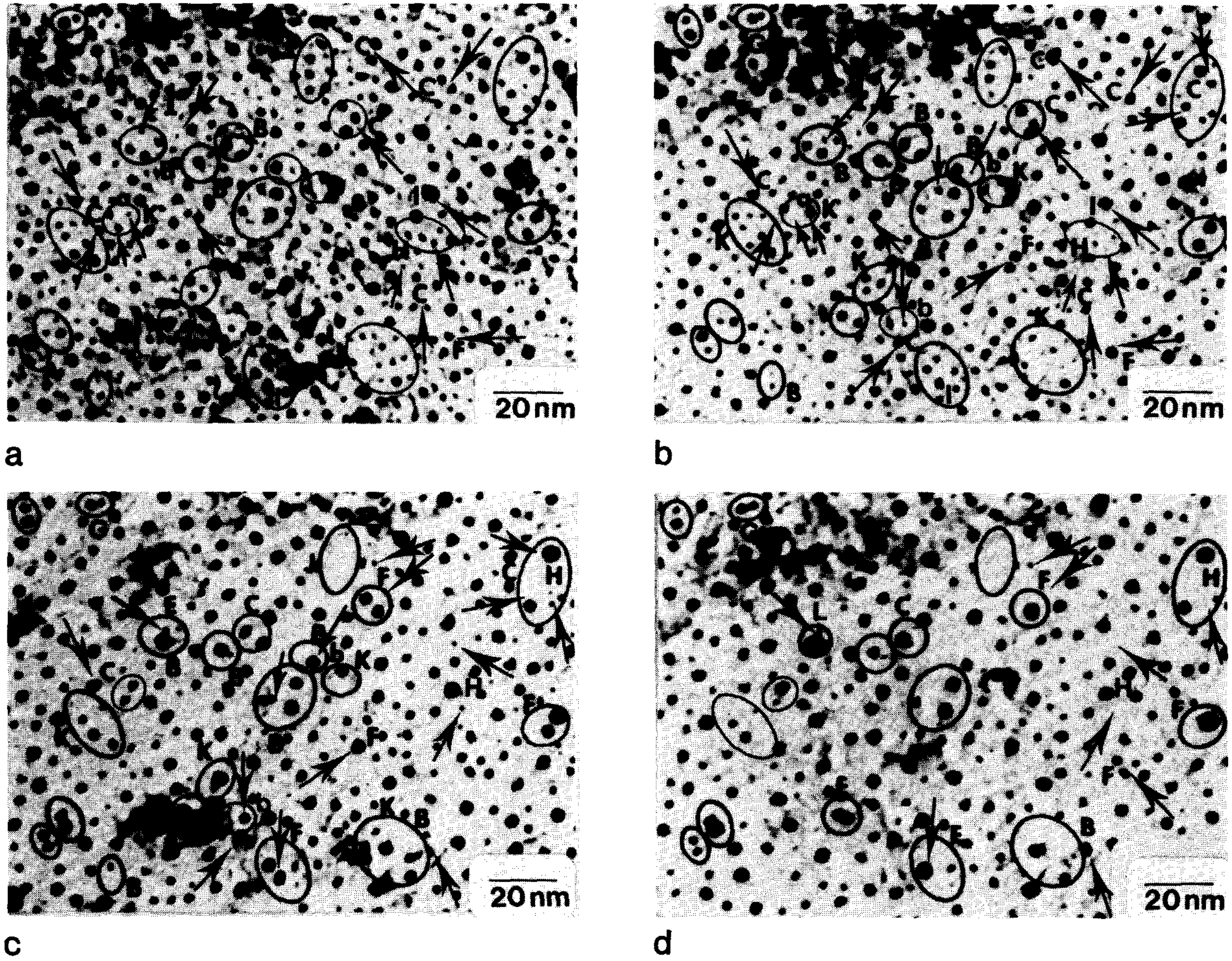
a
b
c
d
20nm
20nm
20nm
20nm

ple with an initial film thickness of 1.5 nm heated in as-received ultrapure hydrogen. The letters on all the micrographs correspond to the respective events listed in Table 1. When the metal-deposited sample was heated in H$_2$ for 6 h at 500°C, detectable particles in the range 0.8–5 nm formed, with the average around 2 nm. The sample with this initial distribution was heated subsequently in the following cumulative sequence: 1, 2, 3, 4, 6, 8, 12, 17, 29, 43, and 65 h. Following the initial 1 h heating, a number of neighboring particles, especially the larger ones, coalesced, decreasing the particle number density (B, C, F in Figs. 1a–1d). A number of small particles 0.8–1.5 nm in size remained unaffected while a number of other small particles decreased in size or disappeared (regions 1 and H in Figs. 1a–1d and 1′a–1′d, for example). All the large particles also appear to have decreased slightly in size (I in Figs. 1a and 1b, for example). Since, as just mentioned, a number of small particles on the substrate remained unaffected, the decrease in the size of the large particles may be a result of emission of atoms to the substrate, due not to a global ripening mechanism, but more likely to local variations in curvature along the periphery of the large particles. Or, it may be a result of extension of an undetectable film from around the particles or of diffusion of material into the substrate. It may also be a result of mere reconstruction with time to a more compact shape. During the next three 1-h intervals of heating, the number of particles decreased further. Both the decrease and disappearance of smaller particles (H, J) and the coalescence of nearby particles in the vicinity of unaffected or decreasing smaller particles were observed (C, F in Figs. 1b–1d). Also, a number of nearby

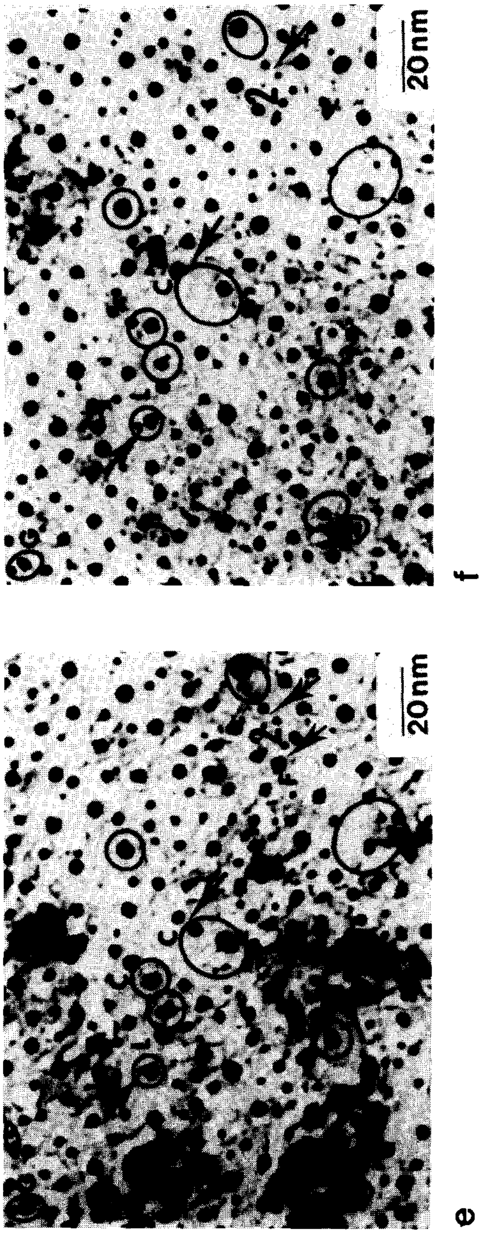

FIG. 1. Sequence of changes in the same region of a Pt/Al$_2$O$_3$ sample of 1.5 nm initial film thickness on heating in as-supplied hydrogen at 500°C. The following durations of heating, starting with (b), are cumulative. (a) Initial (6 h H$_2$); (b) 1 h; (c) 2 h; (d) 4 h; (e) 17 h; (f) (65 h H$_2$ +) 16 h O$_2$.

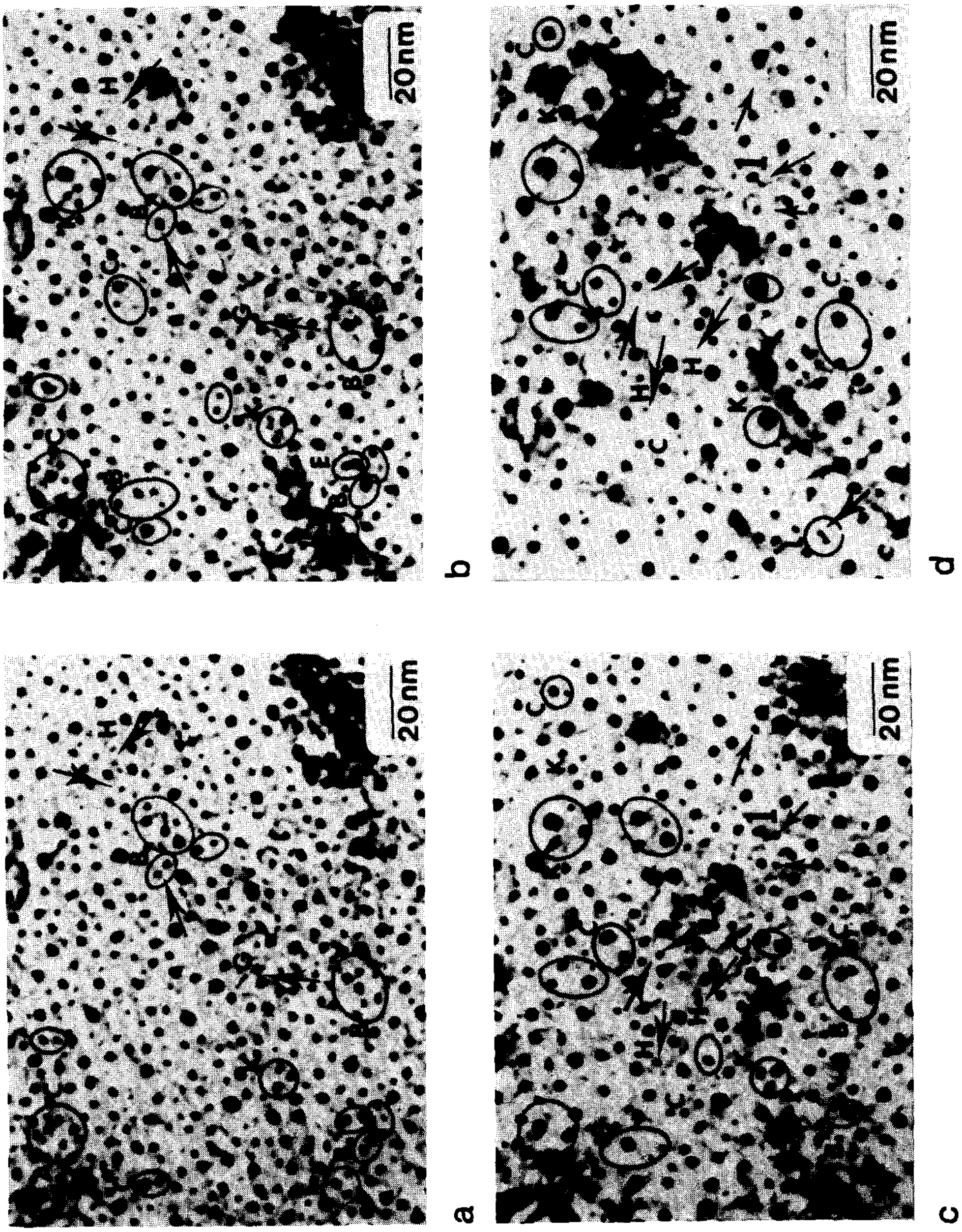
a
b
c
d
20 nm
20 nm
20 nm
20 nm
A
B
C
D
E
G
H
K

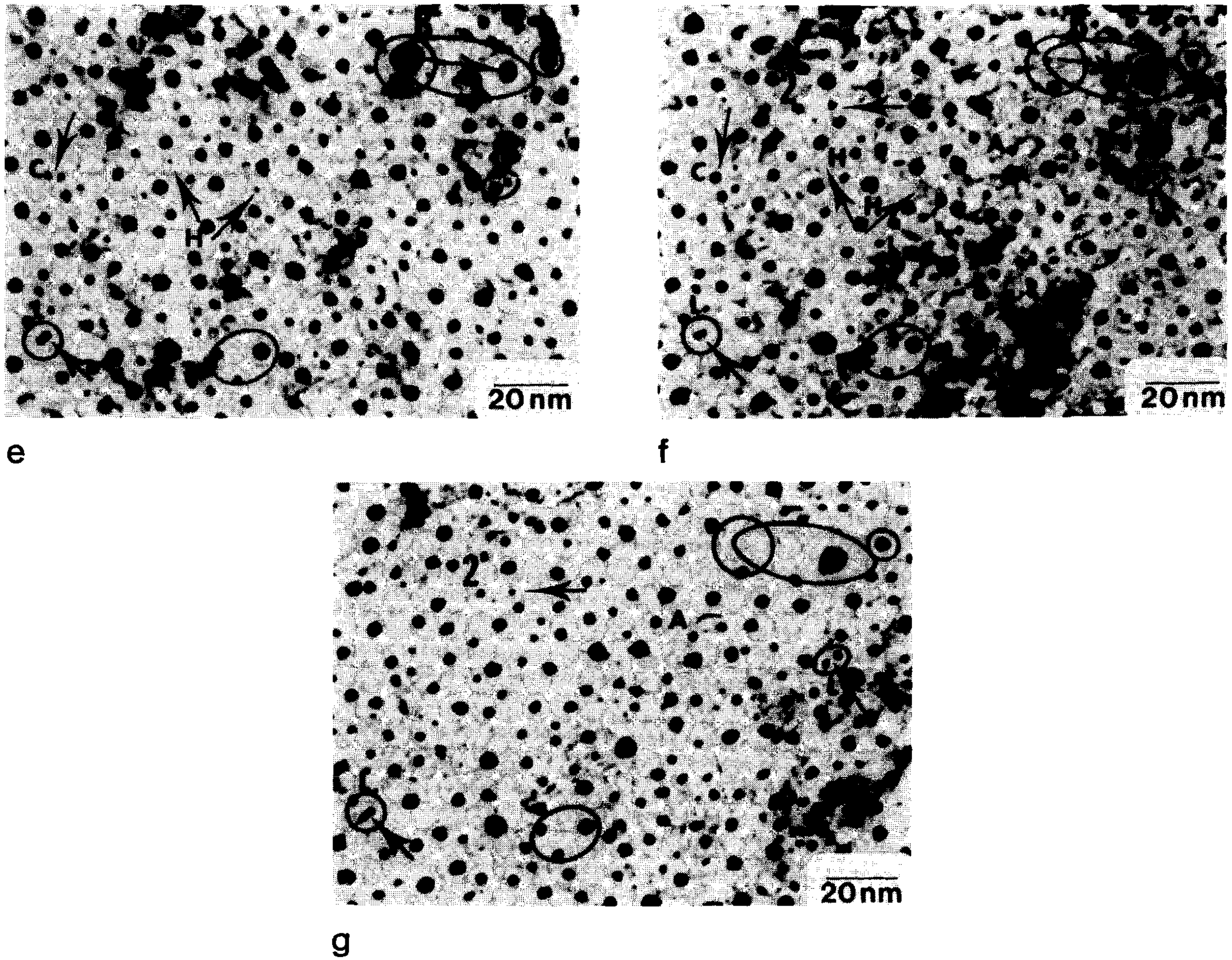

FIG. 1′. Same sample as in Fig. 1. The micrographs are of a different region. (a) Initial (6 h H_2); (b) 1 h; (c) 2 h; (d) 12 h; (e) 29 h; (f) 65 h; (g) 16 h O_2.

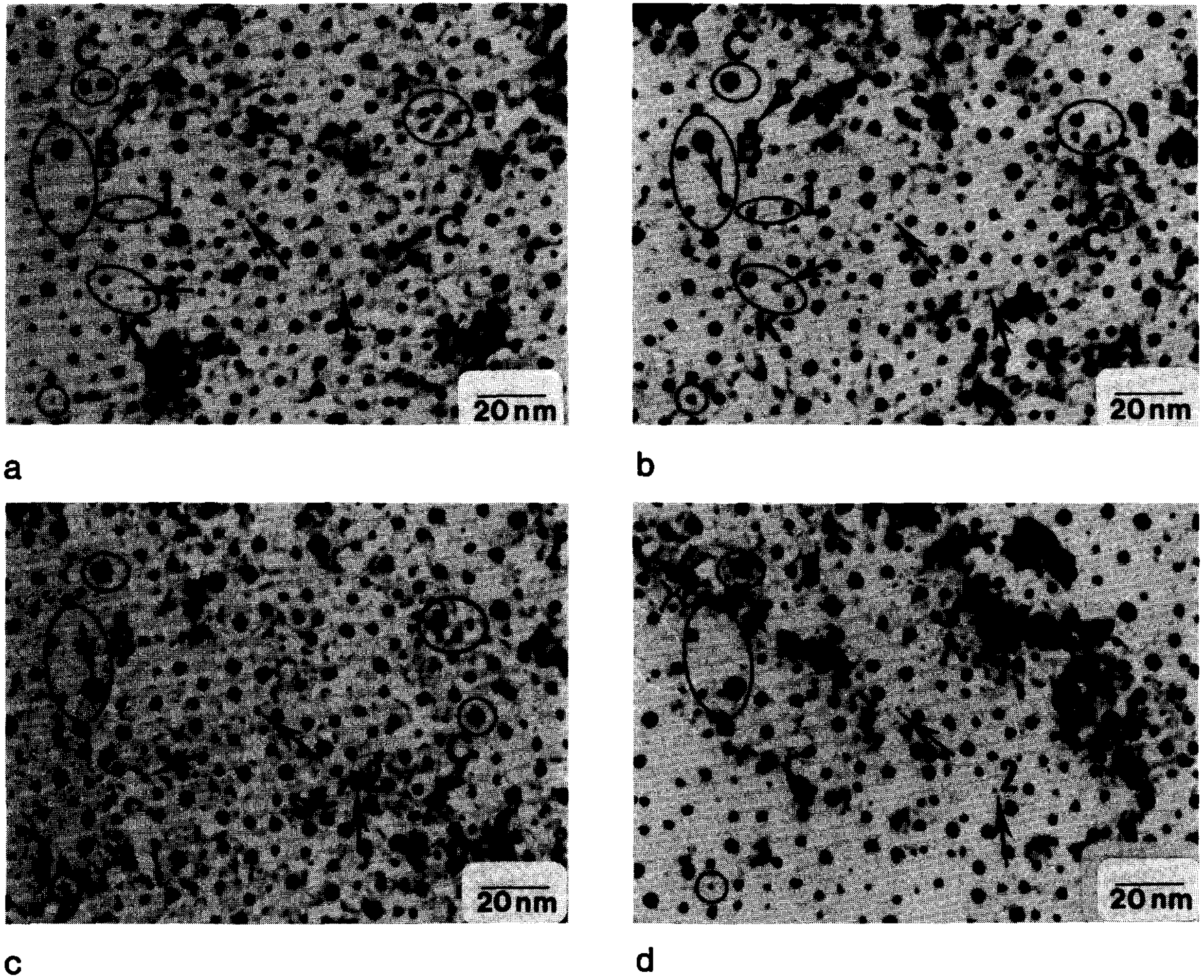

FIG. 1″. Same sample as in Fig. 1. The micrographs are of yet another region. (a) 6 h H_2; (b) 29 h H_2; (c) 65 h H_2; (d) 16 h O_2.

small particles appear to have coalesced to form larger particles (K); this growth occurs either by migration and coalescence of the crystallites or by direct ripening between nearby crystallites, more likely by the former, as the particles are of about the same size and small, ~2 nm (K in Figs. 1b, 1c and 1′b, 1′c). In fact, in the region marked "a" in Figs. 1a and 1b, a small particle (about 0.8 nm) appears to have grown to about 2.5 nm, very likely as a result of the migration and coalescence with it of a larger particle from nearby. A similar event is visible at "b" in Figs. 1b and 1c. The subsequent heat treatment for up to a total of 8 h brought very little change (not all the micrographs for the entire heating sequence are shown here). At the end of a total of 12 h of heating only a few additional pairs of nearby particles had coalesced. However, there was a marginal increase in the size of all the particles, both small and large. Small particles, as small as 1.5 to 2 nm still remained on the substrate. It is possible that all the particles over the entire observable size range could have increased in size marginally at the expense of particles much smaller than about 0.8 nm, either by their coalescence with the migrating crystallites or by a global ripening mechanism. On the other hand, the increase in size may also be a result of extension and/or reconstruction of the particles. Following 17, 29, and 43 h total heating, a number of pairs of large particles coalesced. Very few small particles disappeared. Particles were formed in some places where no particles had been apparent previously (region 1 in Figs. 1″a, 1″b). After heating for additional 22 h (to 65 h of total heating), a number of large crystallites (up to about 8 nm) migrated large distances (up to about 30 nm). Some of these crystallites coalesced with other particles (B in Figs. 1′e, 1′f and in 1″b, 1″c), while some stopped short of colliding (not shown in figures). A number of other particles near each other coalesced, most likely by migration and collision. It is to be noted that long durations of heating lead to significant sintering, especially when the loading is high, though it is not as rapid and pronounced as in the initial stages. During this sequence of heating it was also observed that sometimes two nearby particles made contact via a faint, narrow neck or a whiskerlike bridge. The particles then either sintered via a transfer of atoms along the bridge or separated again as the interconnecting bridge was broken (G in Figs. 1b–1f and 1′a, 1′b). In some cases the two particles more or less completely coalesced and then tended to separate again (L in Figs. 1d–1f and 1′b–1′g). Additional events observed are marked on the micrographs by various letters corresponding to the events listed in Table 1.

When the above sample was subsequently heated in O_2 at 500°C for up to 28 h, no particle migration or detectable ripening of particles was observed. However, most of the particles, small and large, decreased in size (region 2 in Figs. 1f, 1′g, and 1″d) as a result of either emission of atoms/molecules to the substrate or of the extension and formation of films undetectable by electron microscopy around the particles. This phenomenon is discussed further in Refs. (*57, 58*). Two additional cycles of heating in H_2 and O_2 for a total of 50 h resulted in marginal particle coarsening mostly via coalescence of neighboring particles (C in Figs. 2a–2b). Particle migration without coalescence (A in Figs. 2a, 2b) and elongation of some particles (O in 2a, 2b) could also be observed. Almost all the detectable particles of about 0.8 nm and even less remained (some of them are marked with arrows in Figs. 2a, 2b). Following subsequent cycles of alternate heating in H_2 and O_2, a large number of events of migration and coalescence of particles (A, B in Figs. 2c–2f and 2′a–2′e) and dumbbell-shaped particles (E in Figs. 2e–2f and 2′a–2′e) could be observed in both O_2 and H_2, as shown in Figs. 2 and 2′. As seen on the micrographs (Figs. 2 and 2′), there is, in addition, a marginal decrease in the size of all the particles on heating in oxygen and an increase in size on

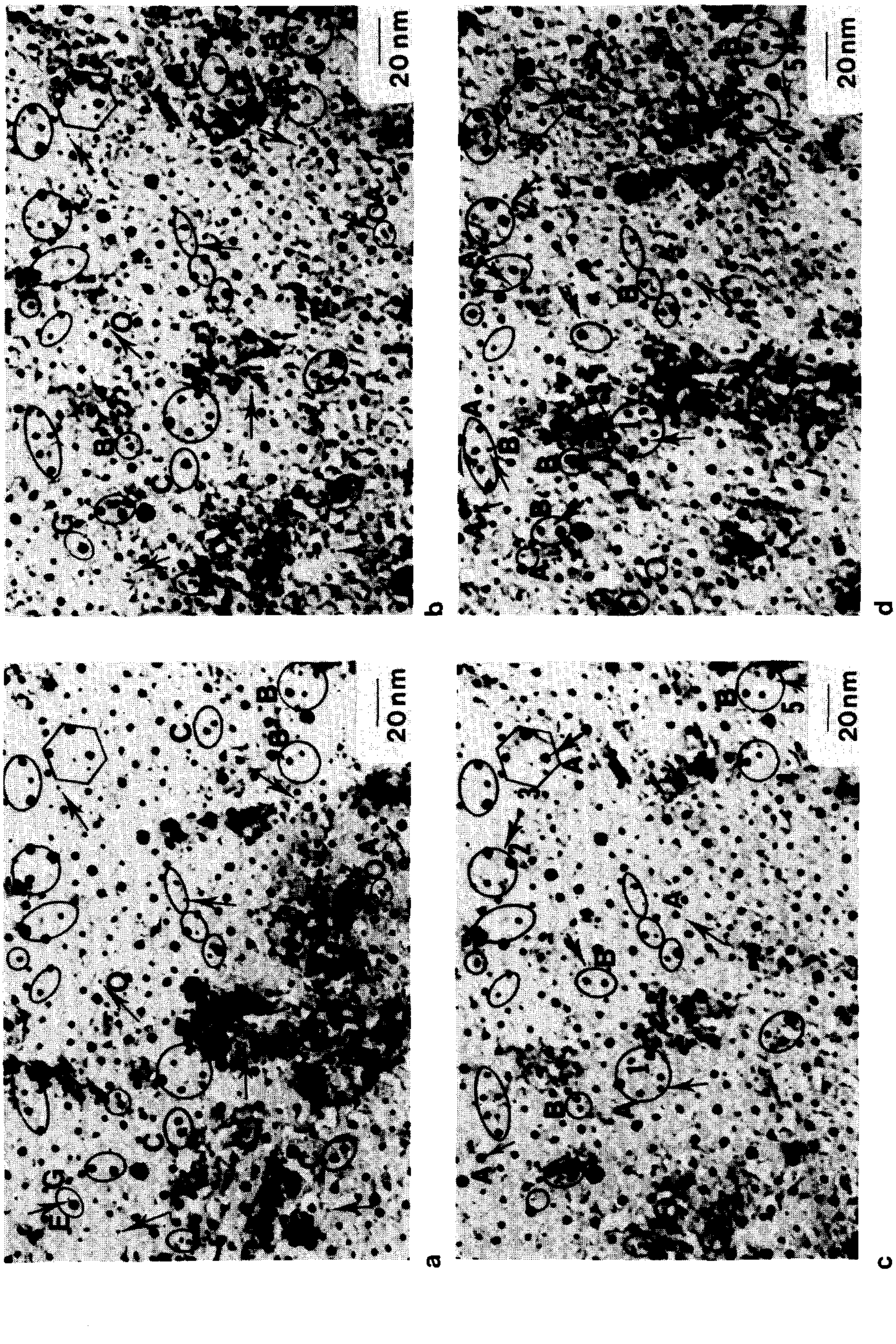
a
b
c
d
20 nm
20 nm
20 nm
20 nm

heating in hydrogen (Figs. 2c and 2d), which is discussed in detail in Refs. (*57*, *58*). It can be seen that while there is very little ripening, especially of the global kind, large particles (regions marked 1–5 in Figs. 2c–2f and regions 1 and 2 in Figs. 2′a–2′e), as large as 8 nm (region 1 in Figs. 2′a–2′e), migrate gradually over large distances (25 nm) and coalesce with other particles. At region 2 in Figs. 2e and 2f, the large particle appears to have migrated over a smaller particle. The smaller particle is probably trapped in a valley on the substrate surface and does not hinder the migration of the larger particle over it. On the other hand, at region 1 in Fig. 2′, for example, the large particle incorporates into itself the smaller particles it encounters while migrating. The numerous events marked A, B, and E in the micrographs provide evidence for more than isolated incidents of crystallite migration in supported model catalysts. Also, dumbbell-shaped particles (E in Figs. 2 and 2′) remain over extended periods of heat treatment, suggesting that coalescence can be a rate-limiting step. This is in contrast with the suggestion that coalescence must be fast (*14*). In addition, as noted before, sometimes two neighboring particles collide, partially coalesce, and then separate into two again (L in Figs. 2e, 2f and 2′d, 2′e).

It is clear that migration and coalescence play a role in the coarsening of Pt/Al$_2$O$_3$ catalysts not merely during the initial stages of sintering of a fresh sample but also after prolonged heat treatment of the sample. In contrast to the opinion that especially in an oxidizing atmosphere only atomic/molecular migration takes place, the present results show that migration and coalescence of crystallites also occur.

From the above results one can note that when an already sintered sample is heated

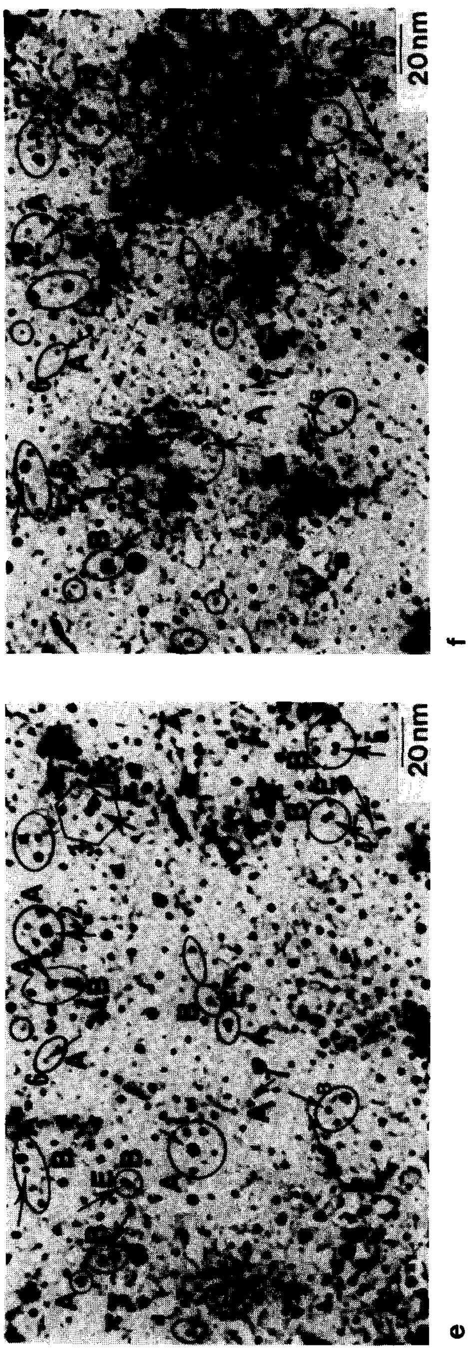

FIG. 2. Same sample as in Fig. 1 heated subsequently in H_2 and O_2 alternately at 500°C. (a) Initial (65 h H_2 + 28 h O_2 + 18 h H_2 + 14 h O_2); (b) 6 h H_2; (c) 12 h O_2; (d) 14 h H_2; (e) 12 h O_2; (f) 10 h H_2 + 10 h O_2.

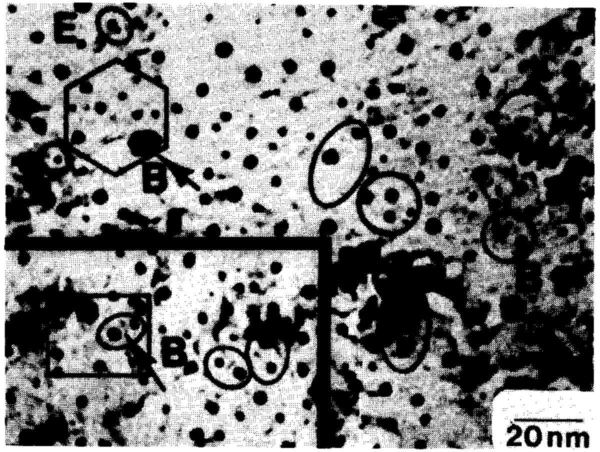

a

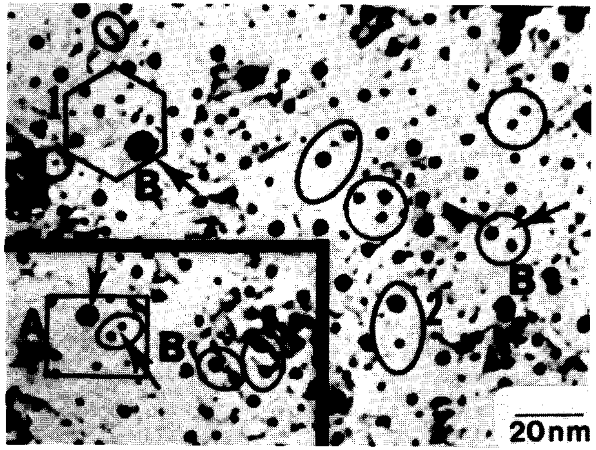

b

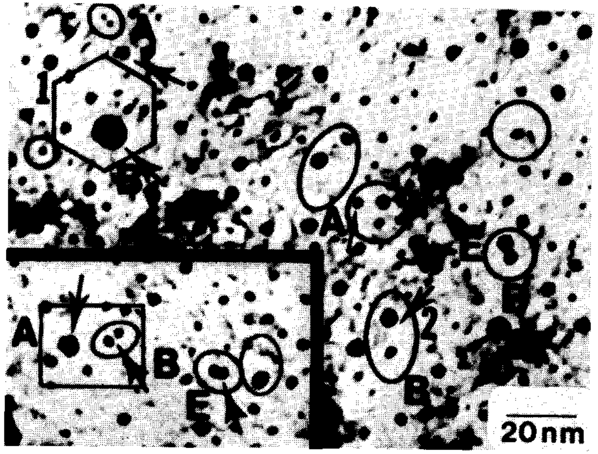

c

further, changes begin to occur after two or three cycles of alternate heating in H_2 and O_2. Very little change with regard to sintering is noticed on extended heating in the same atmosphere. A change in exposure, either of an oxidized sample to a reducing atmosphere or of reduced particles to O_2, brings about particle motion, coalescence, etc. This is perhaps due to the heat of reaction involved, as suggested also by Glassl *et al.* (*33*). The above results show that migration of particles in Pt/Al_2O_3 catalysts occurs at the relatively low temperature of 500°C, both with a fresh sample in H_2 and a "sintered" sample in both O_2 and H_2.

A different sample of 2-nm initial film thickness was heated in additionally purified H_2 at 500°C for 12 h and subsequently at 600°C for 5 h to generate particles. Following heating at 500°C, a large number of particles of about 1.6 nm average size were formed. The specimen employed in the experiments described in the previous paragraphs, which had a lower metal loading of 1.5-nm initial film thickness, yielded slightly larger particles following only 6 h of heating at 500°C. The difference in the sintering behaviors of these two specimens points to the role of the type of hydrogen used. Sintering is faster and relatively more pronounced in the as-received hydrogen (which contains traces of water) than in the further purified H_2. Similar trends were also observed by Smith *et al.* (*41*). The additional heating at 600°C for 5 h caused severe sintering. Dumbbell-shaped particles could be observed following both the 500 and the 600°C heat treatments (particles marked with arrows in Figs. 3a and 3b). Even though the sintering mechanism could not be followed during these heat treatments because of the severity of sintering, the presence of dumbbell-shaped particles

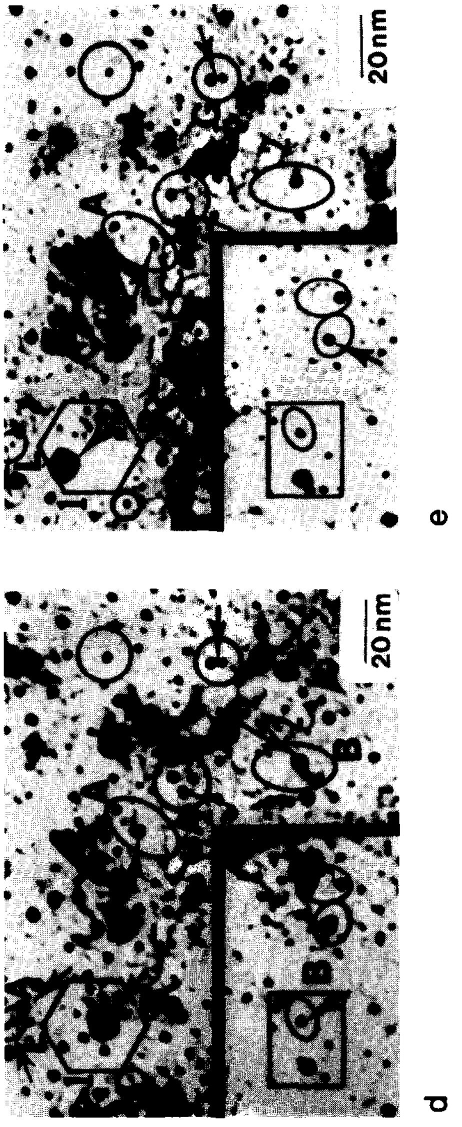

FIG. 2'. Same sample as in Fig. 2. The micrographs are of a different region. (a) Initial (same as in Fig. 2); (b) 6 h H_2; (c) 12 h O_2 + 14 h H_2; (d) 12 h O_2; (e) 10 h H_2 + 10 h O_2. The regions bounded by the black margins are from a different area.

suggests that at both temperatures crystallite migration and coalescence were involved. This sample was subsequently heated alternately in O_2 and purified H_2. A few select micrographs are shown in Figs. 3′ and 3″. The heat treatment in O_2 was carried out from 300 to 500°C, with a 50°C increment in successive cycles. But the heat treatment in H_2 in each cycle was carried out at 500°C. (The incremental heating in O_2 was carried out in an attempt to identify the lowest temperature at which film formation around the particles, or a decrease in size of all the particles, occurs. Film formation around particles when Pt/Al_2O_3 model catalysts are heated in O_2 is discussed in Refs. (*57, 58*).) Throughout this treatment and especially up to the 500°C O_2/H_2 cycling, the growth was slow and gradual and the marginal growth occurred mostly by coalescence of nearby particles (C in Figs. 3′b–3′f). However, at 500°C, as with the other sample reported in the previous paragraphs, significant migration and coalescence were observed on alternate heating in H_2 and O_2. A number of particles as small as 1 nm remained with very little change throughout the various cycles of heating for up to a total of about 100 h (some are marked with arrows in Figs. 3′a–3′f and 3″a–3″h), while a few others disappeared. This suggests that at low temperatures very little global ripening, involving a large number of particles, takes place (in spite of the alternating oxidizing and reducing treatments). Particle migration (A), migration and coalescence (B and C in Figs. 3′ and 3″), and direct ripening between a small and a larger particle via a narrow whiskerlike bridge (G, region 1 in Fig. 3″) were all observed. In other cases nearby particles made and broke contact a few times without any change in the size of the particles (region 2 in Fig. 3″). These events indicate that in some cases the coalescence is retarded or inhibited altogether and that coalescence may also be a rate-limiting step, as stated before.

Another sample from the same batch as the preceding one with a 2-nm initial film thickness of Pt was heated similarly in purified H_2 at 500°C for 12 h and subsequently at 600°C for 5 h to obtain an initial crystallite distribution (Fig. 4a). Heating this sample further in purified H_2 at 700°C for only $\frac{1}{2}$ h led to severe sintering (Fig. 4b). A large number of small and relatively large particles disappeared, other particles of the same size and even smaller remained unaffected, while some of the smaller particles also decreased in size (particles marked with arrows in Figs. 4a, 4b). In addition, a large number of neighboring pairs of crystallites coalesced, as indicated by the elongated and/or dumbbell-shaped particles in the micrographs (C, E in Figs. 4a, 4b). In one location, out of the two small particles adjacent to a much larger particle, the seemingly larger of the two decreased in size while the smaller grew or remained unaffected (regions 1, 2 in Figs. 4a–4d). In another place, two large particles of about the same size coalesced into one, while the nearby very small particles decreased only slightly in size (F in Figs. 4a–4d). This indicates that both local ripening and short-distance migration and coalescence occur adjacent to each other. Probably because of the high temperature, most of the particles were faceted and rectangular. Subsequent heat treatment at the same temperature for up to a total of 5 h resulted in gradual sintering, and similar events such as coalescence of neighboring particles (C), decrease in size of small particles (H), decrease in size and migration (D), gradual migration and coalescence (B), and disappearance of small particles (particles marked with arrows) could be observed (Figs. 4b–4d). Also, the particles became relatively circular. Heating this sample further in H_2 at 800°C for 2 h led to a drastic decrease in the number of particles and an increase in the average particle size. A large number of both small and large particles disappeared (J and particles marked with arrows in Figs. 4d, 4e). Some relatively large particles decreased in size while considerably smaller

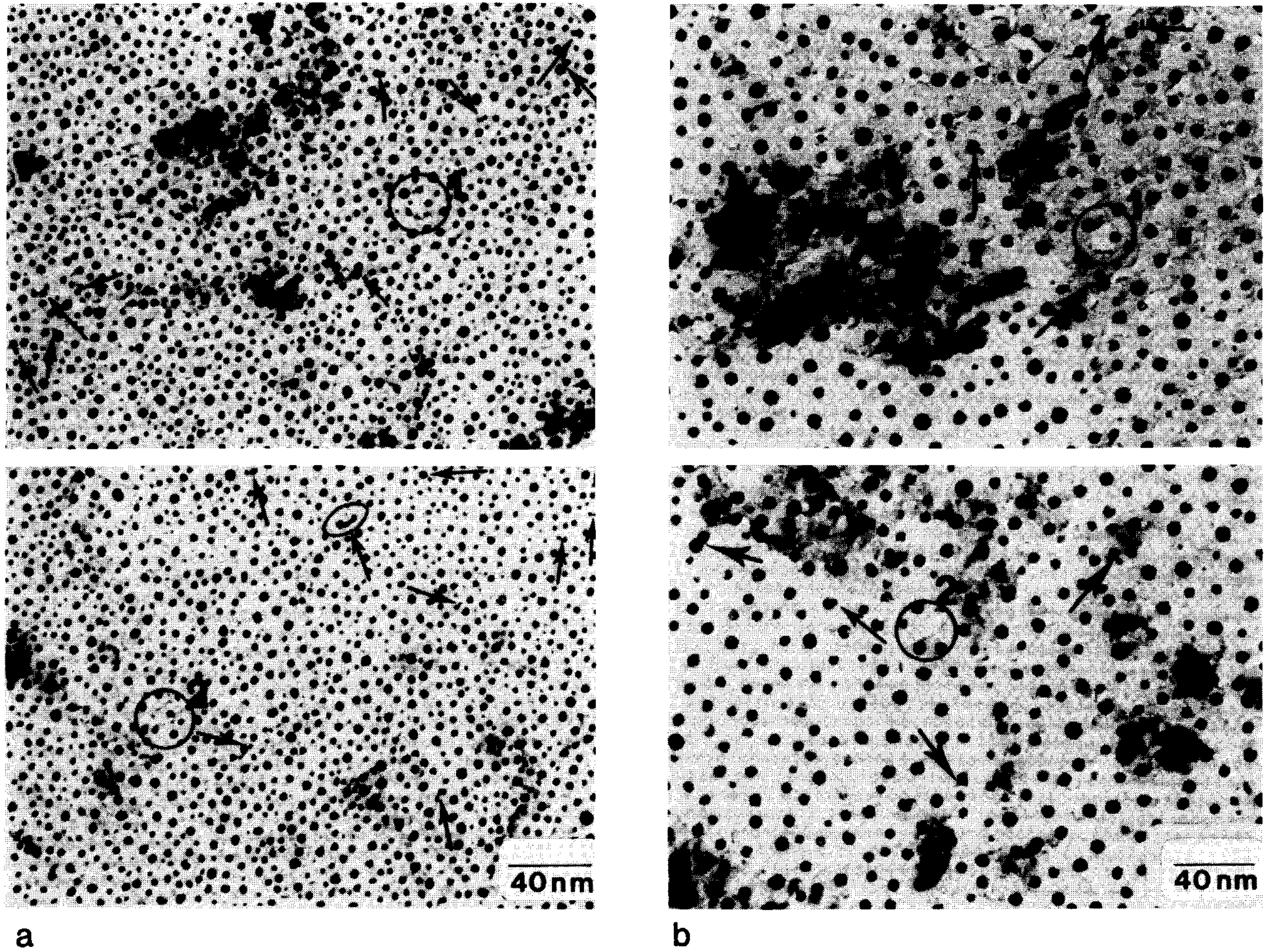

FIG. 3. Changes on heating a Pt/Al$_2$O$_3$ sample of 2 nm initial film thickness in purified hydrogen. The micrographs are of the same regions. (a) 12 h H$_2$, 500°C; (b) 5 h H$_2$, 600°C.

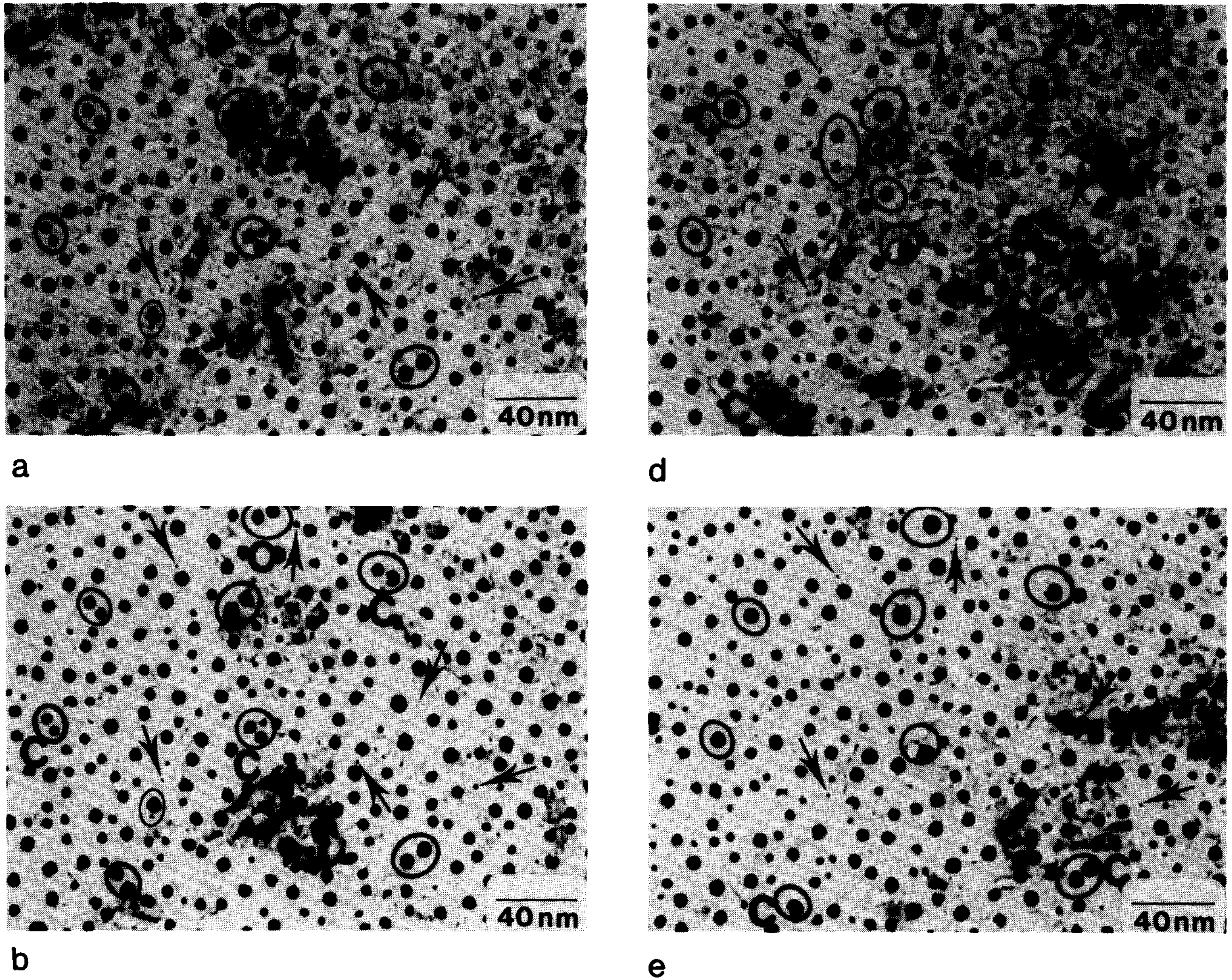
40nm
a
40nm
d
40nm
b
40nm
e

particles nearby remained unchanged (I). The sintering was very fast and it can only be inferred that both short-distance migration and subsequent coalescence of particles (B, C) and localized ripening (H) and migration of smaller particles, which decreased in size as they migrated (regions 1, 3 in Figs. 4d, 4e), contributed to the growth of the particles.

Another sample of 1.5-nm initial film thickness was heated in purified H$_2$ at 750°C for 1 h to generate crystallites. Only 1 h of this high-temperature treatment of the fresh sample with a lower loading (1.5 nm) yielded particles considerably larger than those obtained with a sample of higher loading (2 nm) after 12 h of heating at 500°C. As expected, the sintering is faster and more pronounced at the higher temperatures. Further heating in purified H$_2$ at 750°C for $\frac{1}{2}$ h led to a drastic decrease in the number of particles. The average size of the particles also decreased. The decrease in the number of particles and also an overall decrease in their size cannot possibly be attributed to sintering by a global ripening mechanism. A part of the crystallites is lost via evaporation, or more likely has diffused onto or into the substrate, or has spread as a thin undetectable film. Figures 5a, 5b, 5′a and 5′b show some of the events. A large number of small and large particles disappeared completely without significant growth of the remaining particles (J). In fact, in some locations, the large particles decreased in size significantly while much smaller particles adjacent to them were affected only marginally or even remained unchanged (I). Larger particles were detected in regions where there were smaller particles before, suggesting growth by collision and coalescence of smaller particles (K). Small particles could be seen in re-

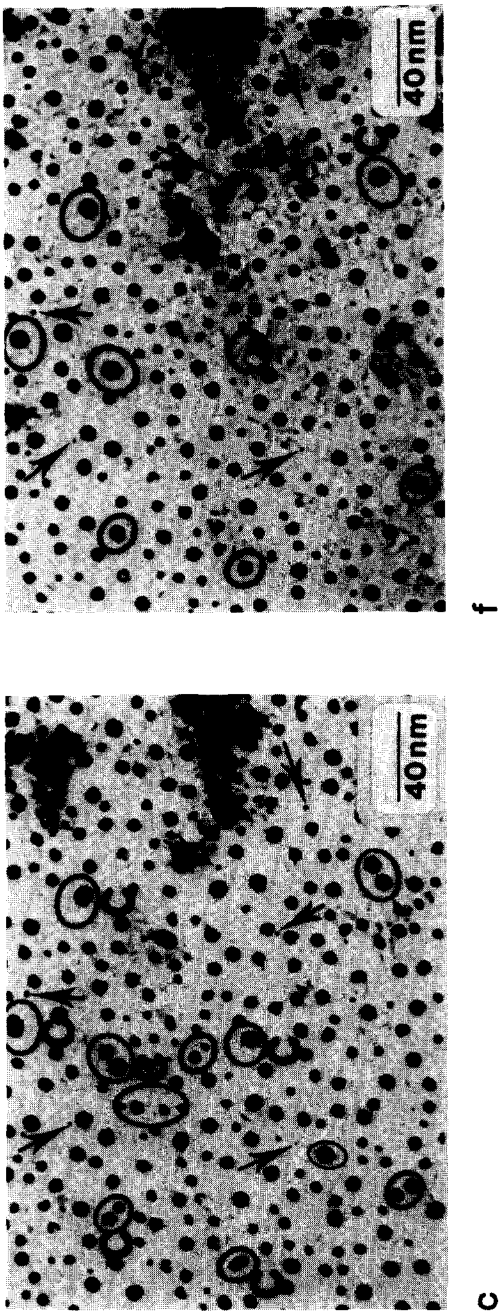

FIG. 3′. Sequence of changes in a different region of the same sample as in Fig. 3. (a) Initial (12 h H$_2$, 500°C + 5 h H$_2$, 600°C); (b) 4 h O$_2$, 300°C; (c) 2 h H$_2$, 500°C; (d) 4 h O$_2$, 350°C + 4 h H$_2$, 500°C; (e) 3 h O$_2$, 400°C + 4 h H$_2$, 500°C; (f) 5 h O$_2$, 450°C.

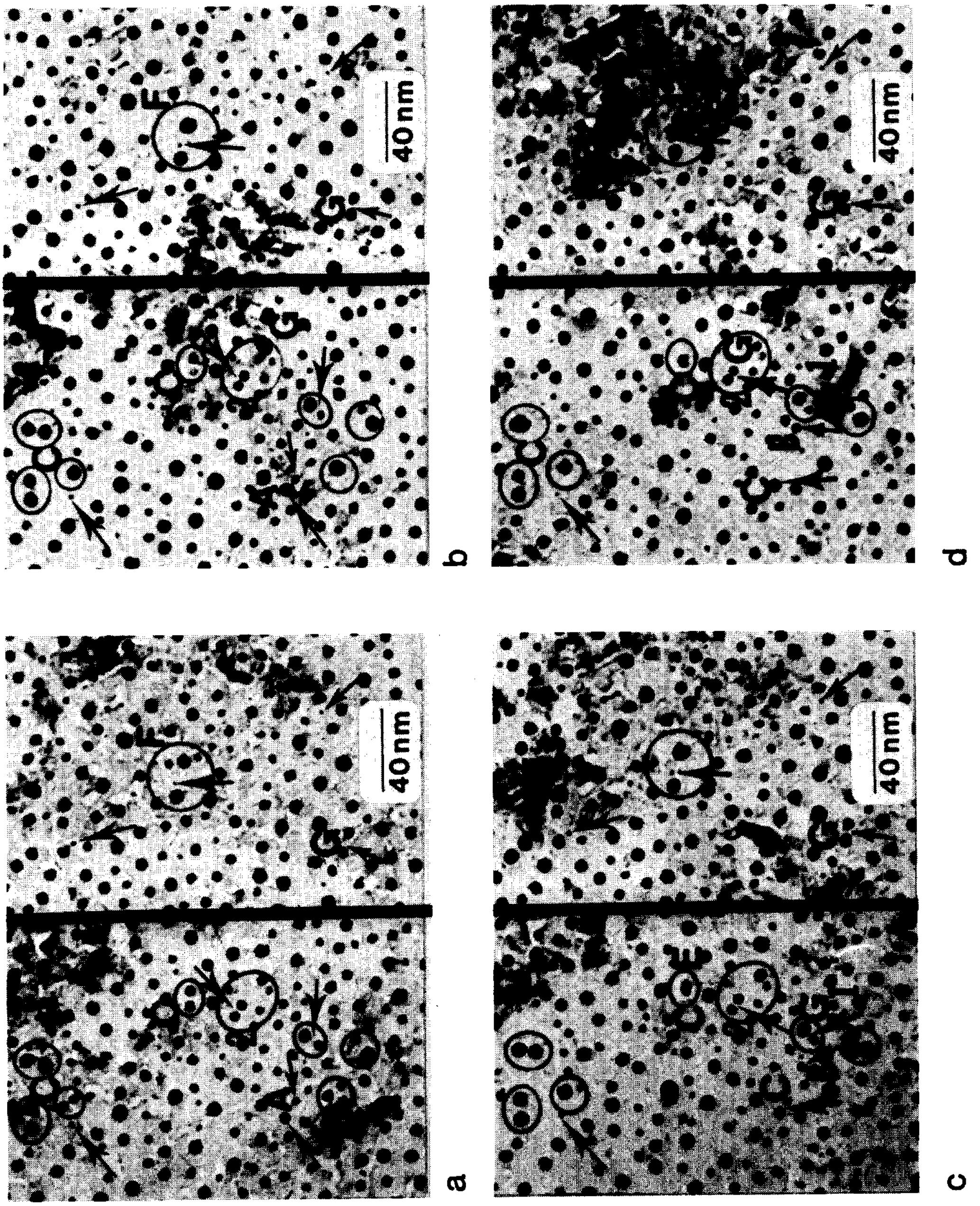
b
40 nm
F
G
d
40 nm
a
40 nm
F
G
c
40 nm
E
F
G

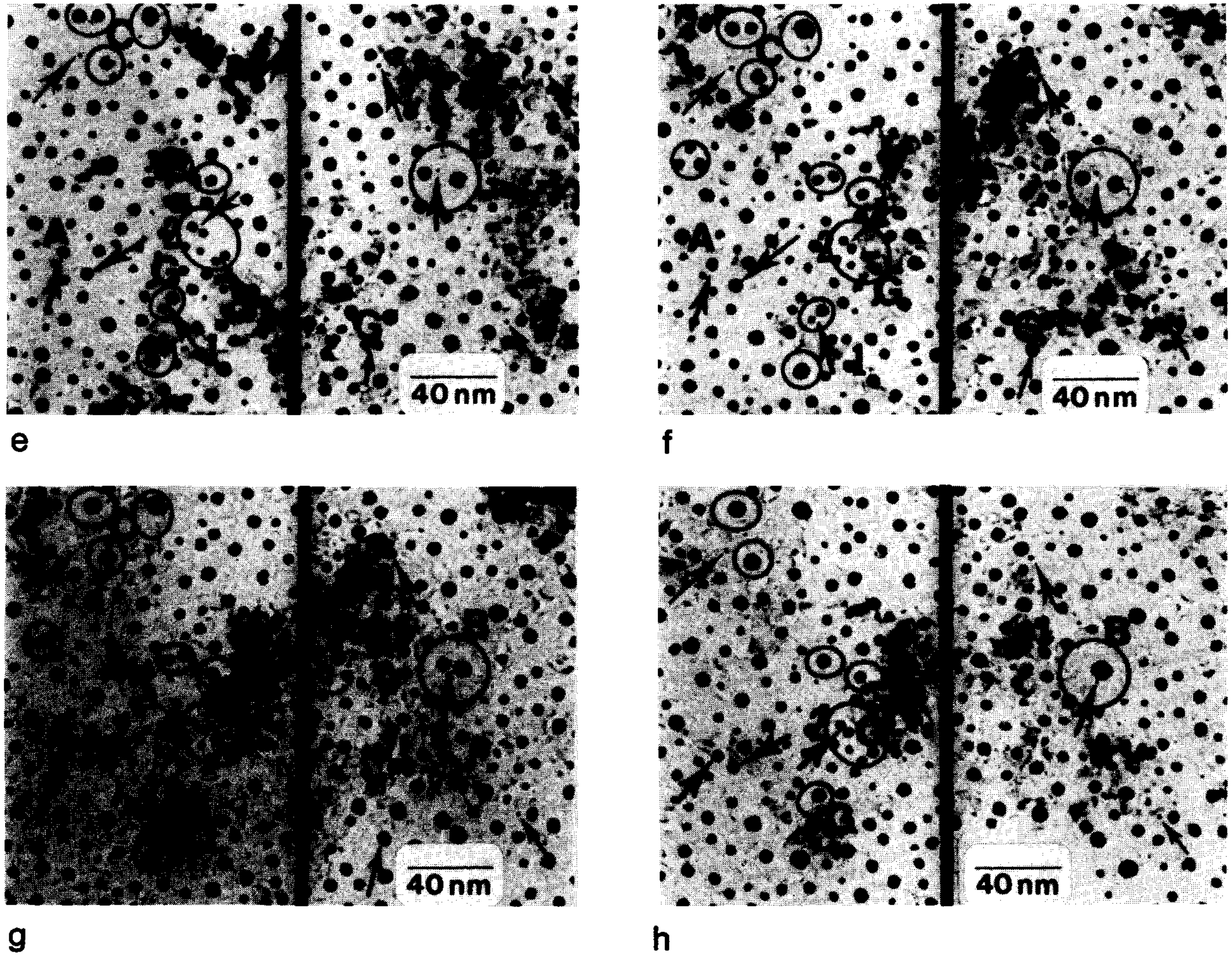

FIG. 3″. Same sample as in Fig. 3. The micrographs are of a different region. (a) Initial (12 h H_2, 500°C + 5 h H_2, 600°C); (b) 4 h O_2, 300°C + 2 h H_2, 500°C; (c) 4 h O_2, 350°C; (d) 4 h H_2, 500°C; (e) 3 h O_2, 400°C; (f) 4 h H_2, 500°C; (g) 4 h O_2, 450°C; (h) 2 h H_2, 500°C.

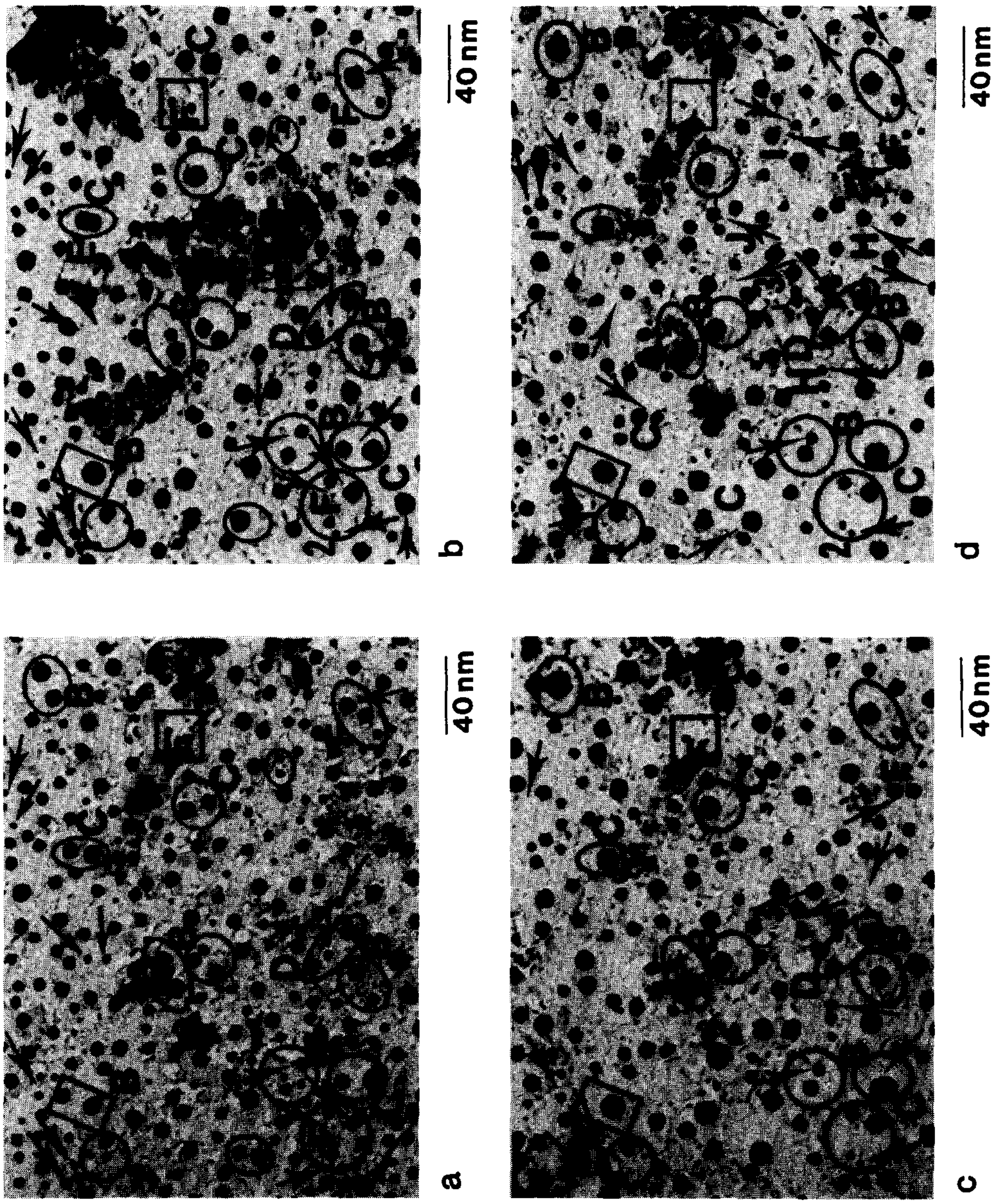
b
40nm
a
40nm
d
40nm
c
40nm

gions adjacent to places where larger particles had disappeared (D), indicating decrease in size and subsequent migration of particles or vice versa. It is unlikely that the new small particles have grown in size from undetectable particles via atom capture because considerably larger particles could be seen to decrease in size or disappear nearby, which is not compatible with the growth of smaller particles from capture of single atoms. It is likely that these particles are migrating remnants of dissolving larger particles. Short distance migration of small particles (~1.5 nm) without coalescence (A) and a few instances of migration with subsequent coalescence (B) could be observed following heating for an additional ½ h at 750°C (Figs. 5′b, 5′c). However, the decrease in the number of particles was very small. Subsequent heating at ½- and 1-h intervals resulted in migration and coalescence of nearby particles (B) (Figs. 5′c, 5′d). A few small particles also disappeared (particles marked with arrows). It is likely that these small particles collided with nearby larger particles and merged with them, since other small particles of about the same size or larger migrated (A) and a few nearby small particles grew (region 1 in Figs. 5′c, 5′d). Beyond 4 h, when longer heating intervals were employed, particle coarsening continued up to a total of 31 h of heating in H_2 (Figs. 5′e–5′g). In addition to coalescence of nearby particles, the decrease in size and/or disappearance of a number of small particles were also observed.

Figure 6 shows another sample heated at 750°C. The micrographs show the events observed on heating in H_2 at 750°C, subsequent to one cycle of heating in H_2 and O_2 at the same temperature. The micrographs show migration of particles (A), particles

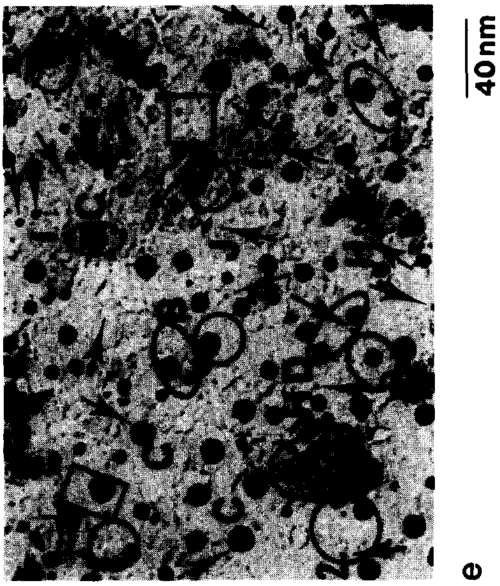

FIG. 4. Sequence changes on heating a Pt/Al_2O_3 sample of 2 nm initial film thickness in purified H_2. (a) Initial (12 h H_2, 500°C + 5 h H_2, 600°C); (b) ½ h H_2, 700°C; (c) 2 h H_2, 700°C; (d) 5 h H_2, 700°C; (e) 2 h H_2, 800°C.

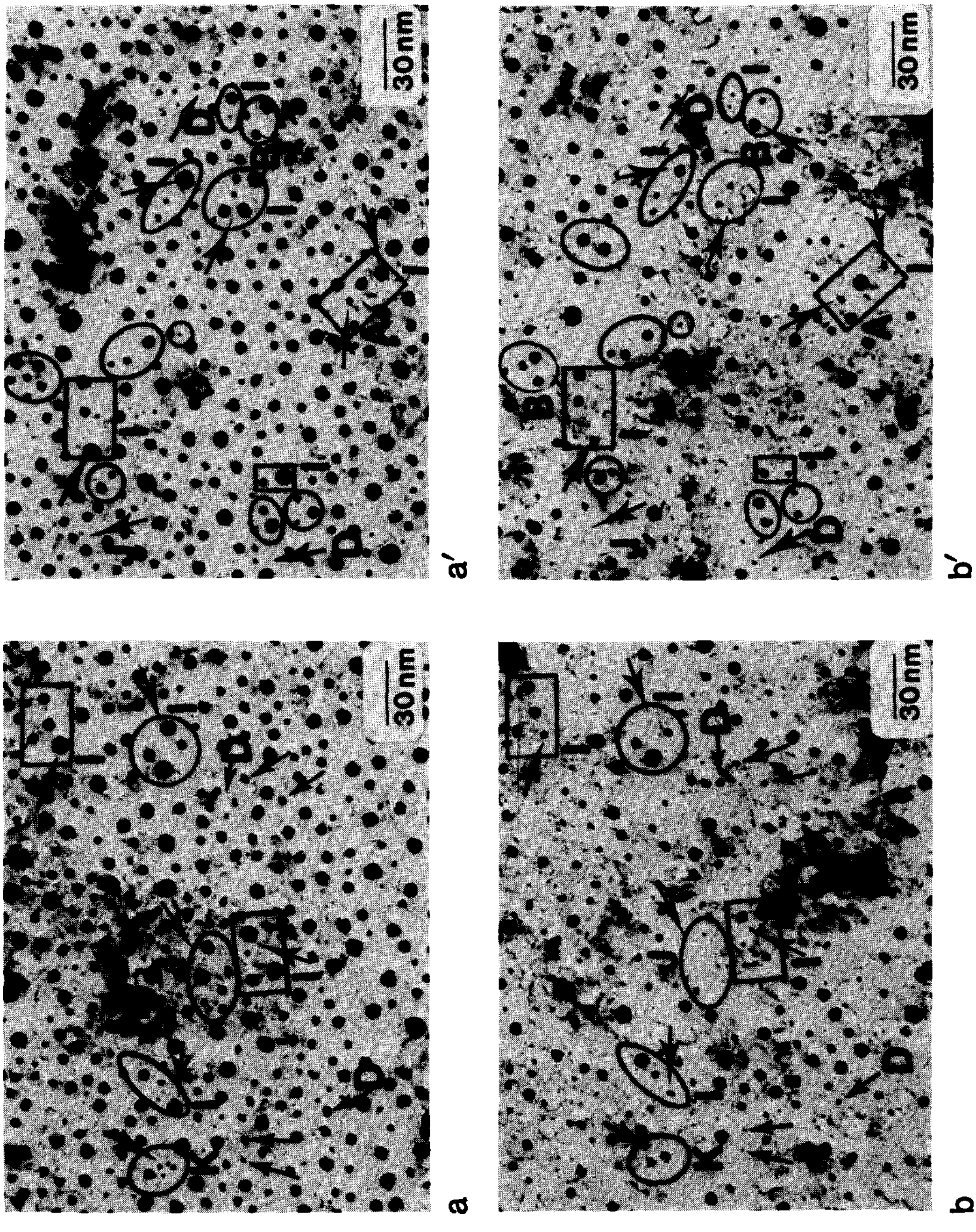

FIG. 5. Micrographs showing the sequence of changes in a Pt/Al$_2$O$_3$ sample of 1.5 nm initial film thickness on heating in purified hydrogen at 750°C. (a, a′) Initial (1 h H$_2$, 750°C); (b, b′) ½ h H$_2$, 750°C.

that were initially apart but later contacted each other, indicating migration and collision (B), dumbbell-shaped particles (E), separation into two of contacting particles (L), and generation of two particles from one (M). Also, a number of instances of overlapping particles (N) could be seen.

DISCUSSION

The results reported here have provided further evidence for crystallite migration and coalescence and their contribution to sintering of Pt/Al_2O_3 catalysts in H_2 and on alternate heating in H_2 and O_2. However, as reported before in the case of Pd/Al_2O_3 (*36*) and Fe/Al_2O_3 (*39*), ripening, especially of the localized kind, also often takes place concurrently. In fact, a variety of events takes place during sintering of supported metal catalysts and a few of them observed here in the case of Pt/Al_2O_3 are summarized schematically in Table 1. Even though short-distance migration and coalescence of nearby particles (particles that are one to a few diameters apart) is probably the major mechanism of particle growth, especially in the initial stages, a decrease in size of smaller particles because of localized ripening has also been observed. A number of small particles of about 1.5 to 2 nm in diameter or smaller disappeared. Since, as mentioned in the previous section, a number of particles of similar size remained unaffected or migrated and since larger particles have also been observed to migrate on the same micrograph, there appears to be no compelling reason to attribute the disappearance of such small particles to ripening only. It is possible and quite probable that these particles migrate relatively fast, especially because of their small sizes, and coalesce with the larger particles. Some small particles that remain stationary and unchanged might have been trapped in the valleys of the heterogeneous substrate surface, as also noted previously in the case of Pd/Al_2O_3 (*36*).

It is worth noting that in some cases, two particles approach each other to a kind of distance of minimum approach and growth subsequently occurs via transfer of atoms or molecules from one particle to the other through a very narrow bridge established between the particles (G in Figs. 1′a, 1′b and in Figs. 3″a–3″h). Such a growth by ripening between two adjacent particles via a whiskerlike bridge contact has also been observed with Fe/Al_2O_3 (*39*). It is also possible that the particles coalesce when pulled together because of the contraction of the connecting bridge. Arai *et al.* (*37*) have also postulated that the growth of Pt particles occurs via formation of a bridge between two adjacent particles and coalescence by an abrupt movement that brings the particles together, but only above 600°C and only with particles larger than 10 nm. It appears that when the particles are close to each other, growth via ripening is more of a localized nature, aided by long-range interparticle interactions (which apparently generate a localized curvature that facilitates the removal of atoms or molecules from one particle to the other). In fact, in addition, the micrographs suggest that the migration of crystallites is not diffusional (random) but directional, guided by long-range interparticle interactions. The particles seem to feel the presence of other particles nearby and, in general, migrate toward each other. Of course, migration of particles away from each other has also been observed, though only occasionally. It should be noted that there are also other kinds of interactions affecting the migration of the particles, such as the interactions between particles and support and the surface roughness of the support. Direction-selective migration of particles has been suggested before (*36*). When the interparticle force is strong, it is possible that even if a particle is trapped in a valley or is too large to migrate, it may still rotate and rearrange to orient its more highly curved protrusions along the periphery (and in extreme cases even form long whiskerlike protrusions) in the direction of a nearby particle to emit atoms or molecules toward it (G in Figs.

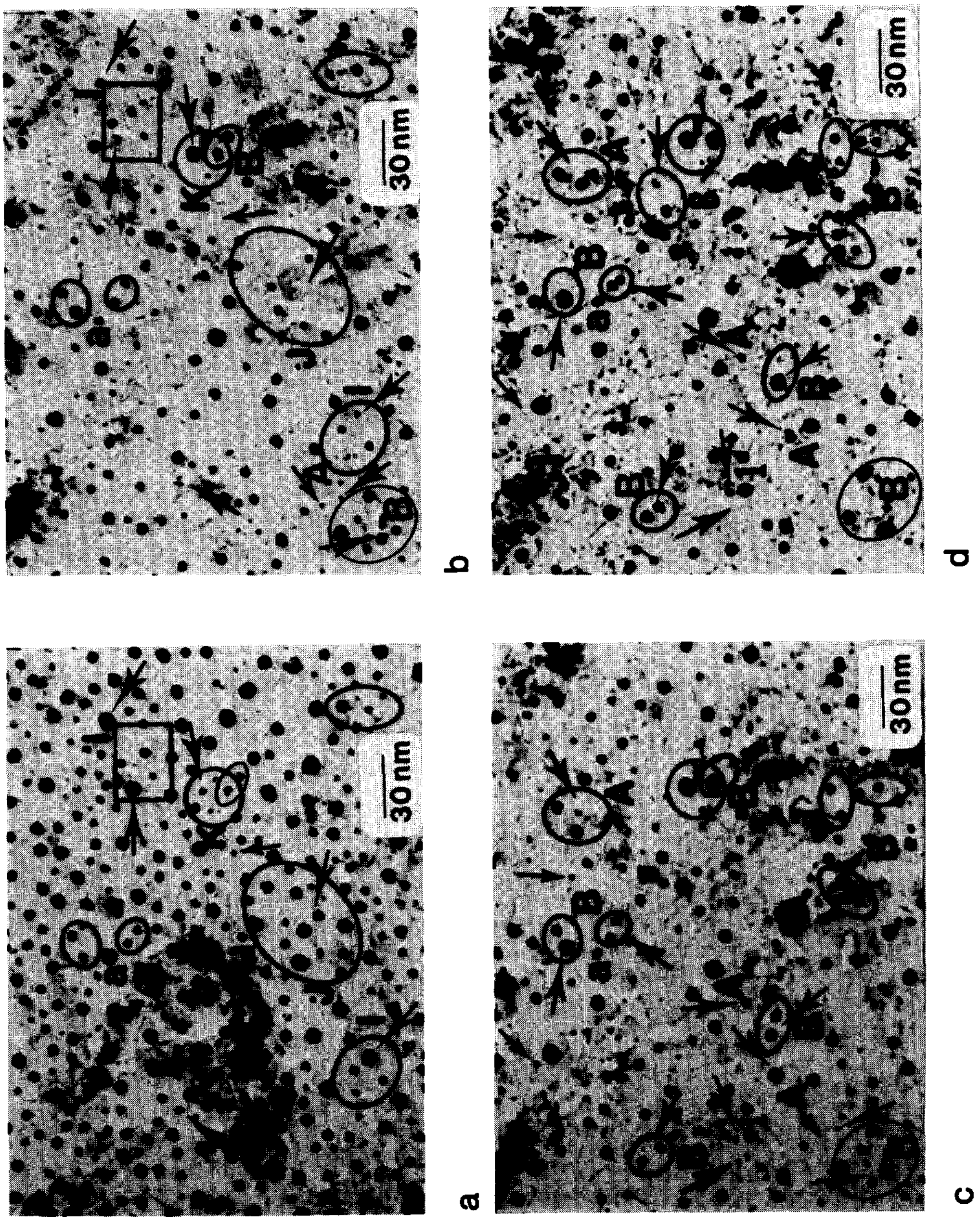
a
b
c
d
30 nm
30 nm
30 nm
30 nm
A
B
K
J
I

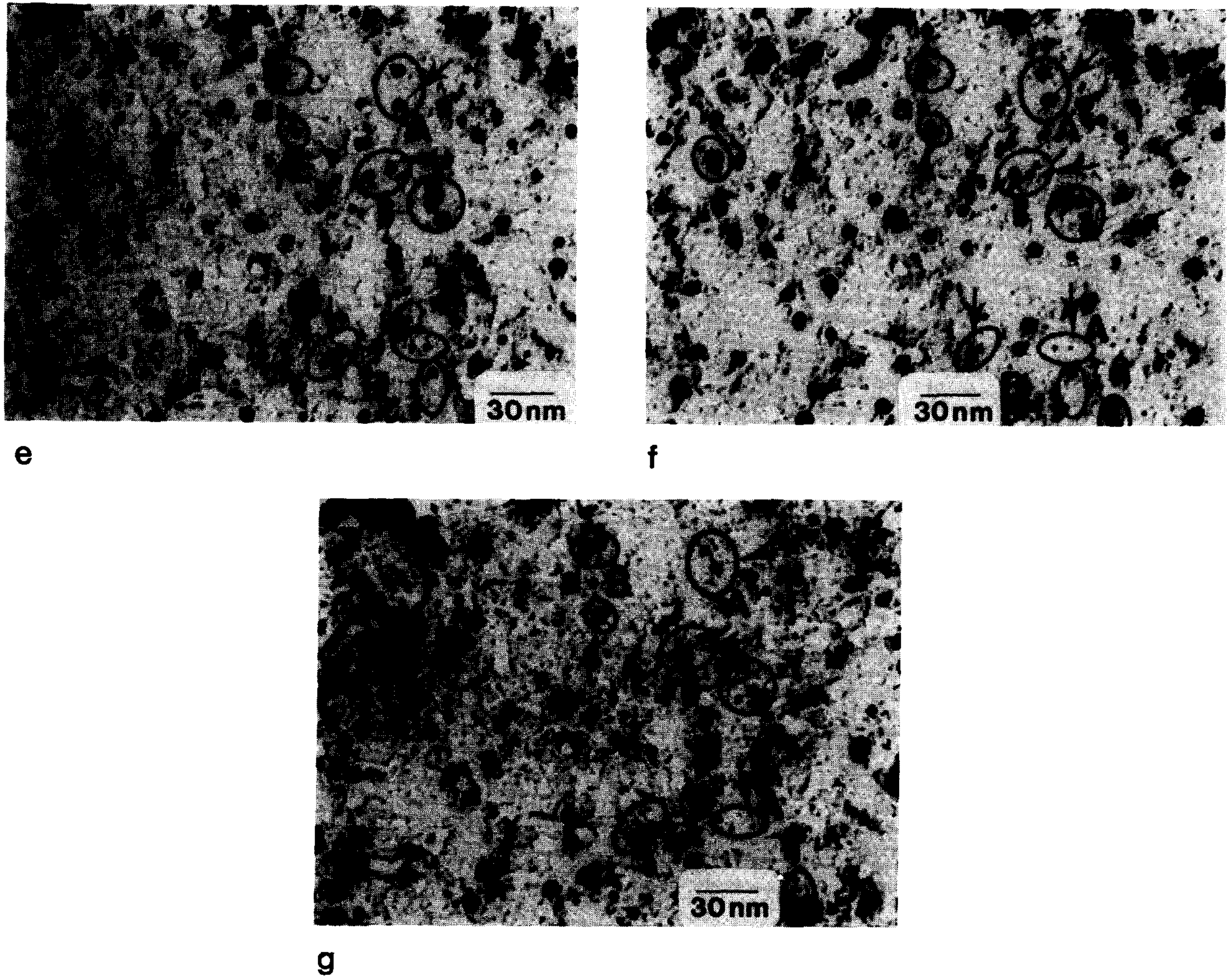

FIG. 5′. Same sample as in Fig. 5. The micrographs are from a region different from those in Fig. 5. The following durations of heating are cumulative. (a) Initial (1 h H_2, 750°C); (b) $+\frac{1}{2}$ h H_2; (c) 1 h H_2; (d) 3 h H_2; (e) 6 h H_2; (f) 9 h H_2; (g) 13 h H_2.

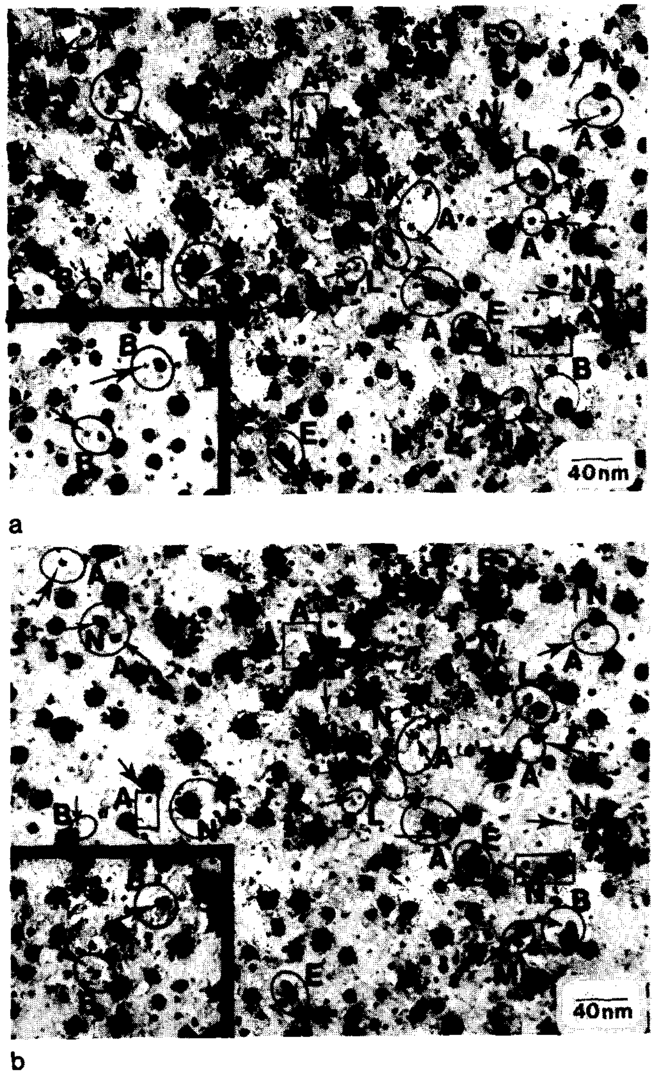

FIG. 6. Sequence of changes in a Pt/Al_2O_3 sample of 1.5 nm initial film thickness heated in purified H_2 and O_2 at 750°C. (a) Initial (15 h H_2, 750°C + 5 h O_2, 750°C + 17 h H_2, 750°C + 6 h H_2, 750°C); (b) 9 h H_2, 750°C.

3″a–3″h). Such events, though isolated, have been observed with Fe/Al_2O_3 previously (*39*). Of course, in the case of supported iron particles the interparticle interaction forces may be stronger because of the ferromagnetic or superparamagnetic nature of the particles.

Finally, there are at least two possible reasons for failure to detect crystallite migration even in systems where it occurs. Since the particles in a fresh sample are, in general, small (less than 1 or 2 nm), they migrate relatively fast and even 1 or 2 h of observation (as is often used) may be too long to identify such a mechanism. Shorter heating intervals, especially in the initial stages, may be helpful. Even in the case of 1 or 2 h of heating, particle migration and coalescence may be detected or inferred if considerable care is taken to follow the same particles in various regions covering a large area of the sample. Second, if the observation is not continued for longer than 1 or 2 h of heating, evidently it is not possible to detect the slower migration of the now relatively larger particles and/or other phenomena that may occur. Also in this case the observation made above regarding careful scanning of a large area might be useful.

In the case of model Pt/Al_2O_3 catalysts, as with other traditional supported metal catalysts, sintering is pronounced at higher temperatures, higher loadings, and at any temperature in the initial few (4–6) hours of heating a fresh catalyst. Sintering in as-received ultrapure hydrogen (which, however, contains traces of moisture and O_2) is enhanced relative to that in the same hydrogen further purified to eliminate/reduce the trace moisture and O_2. In a hydrogen atmosphere and below about 700°C, sintering seems to occur primarily by short-distance migration and coalescence of nearby particles as well as by localized ripening between a few neighboring particles. Significant migration of larger particles occurs around 500°C when H_2-treated samples are heated in O_2 or vice versa. At $T < 500°C$ sintering is very slow in H_2 and on alternate heating in H_2 and O_2 and even slower in O_2.

CONCLUSION

Transmission electron microscopic evidence for the role of crystallite migration and coalescence among other mechanisms in the sintering of model Pt/Al_2O_3 catalysts is provided. Results of model Pt/Al_2O_3 catalysts heated in H_2 and alternately in H_2 and O_2 at temperatures in the range 500–750°C indicate that a large number of phenomena such as coalescence of nearby particles, crystallite migration (of both small, 1.5 nm, and large, about 8 nm, particles), migration followed by coalescence, decrease in size and disappearance of small particles near larger particles, disappearance of small and larger particles, decrease in size of large particles near unaffected smaller particles, decrease in size and subsequent migration of particles or vice versa, collision and inhibited coalescence of particles, and collision–coalescence–separation of particles occur. It appears that the particles on the support feel the presence of nearby particles probably via the interaction forces between them and migrate or emit atoms toward them, and consequently the migration is directional and the ripening is local.

REFERENCES

1. Mills, G. A., Weller, S., and Cornelius, E. B., *Proc. 2nd Int. Congr. Catal., Paris*, p. 2221 (1960).
2. Adler, S. F., and Keavney, J. J., *J. Phys. Chem.* **64,** 208 (1960).
3. Maat, H. J., and Moscou, L., *Proc. 3rd Int. Congr. Catal., Amsterdam* **2,** 1277 (1965).
4. Dalla Betta, R. A., McCune, R. C., and Sprys, J. W., *Ind. Eng. Chem. Prod. Res. Dev.* **15,** 169 (1976).
5. Johnson, F. L., and Keith, C. D., *J. Phys. Chem.* **67,** 200 (1963).
6. Kraft, M., and Spindler, H., *4th Int. Congr. Catal., Moscow,* p. 1252 (1968).
7. Kearby, K. K., Thorn, J. P., and Hinlicky, J. A., U.S. Patent 3,134,732 (1964).
8. Fiedorow, R. M. J., and Wanke, S. E., *J. Catal.* **43,** 34 (1976).
9. Ruckenstein, E., and Malhotra, M. L., *J. Catal.* **41,** 303 (1976).
10. Gollob, R., and Dadyburjor, D. B., *J. Catal.* **68,** 473 (1981).
11. Ruckenstein, E., and Dadyburjor, D. B., *Rev. Chem. Eng.* **1**(3), 251 (1983).
12. Ruckenstein, E., and Pulvermacher, B., *AIChE J.* **19**(2), 356 (1973).
13. Ruckenstein, E., and Pulvermacher, B., *J. Catal.* **29,** 224 (1973).
14. Wynblatt, P., and Gjostein, N. A., *Prog. Solid State Chem.* **9,** 21 (1975).
15. Flynn, P. C., and Wanke, S. E., *J. Catal.* **34,** 390 (1974).
16. Ruckenstein, E., and Dadyburjor, D. B., *J. Catal.* **48,** 73 (1977).
17. Ruckenstein, E., and Dadyburjor, D. B., *Thin Solid Films* **55,** 89 (1978).
18. Flynn, P. C., and Wanke, S. E., *J. Catal.* **37,** 432 (1975).
19. Baker, R. T. K., Thomas, C., and Thomas, R. B., *J. Catal.* **38,** 510 (1975).
20. Hermann, R., Adler, S. F., Goldstein, M. S., and Debaum, R. M., *J. Phys. Chem.* **65,** 2189 (1961).
21. Hughes, T. R., Houston, R. J., and Sieg, R. P., *Ind. Eng. Chem. Process Des. Dev.* **1,** 96 (1962).
22. Gruber, H. L., *J. Phys. Chem.* **66,** 48 (1962).
23. Somorjai, G., *Anal. Chem.* **1,** 101 (1968).
24. Chu, Y. F., and Ruckenstein, E., *Surf. Sci.* **67,** 517 (1977).

25. Chu, Y. F., and Ruckenstein, E., *J. Catal.* **55,** 281 (1978).
26. Chen, M., and Schmidt, L. D., *J. Catal.* **55,** 348 (1978).
27. McVicker, G. B., Garten, R. L., and Baker, R. T. K., *J. Catal.* **54,** 129 (1978).
28. Wang, T., and Schmidt, L. D., *J. Catal.* **66,** 301 (1980).
29. Fiedorow, R. M. J., Chahar, B. S., and Wanke, S. E., *J. Catal.* **51,** 193 (1978); Wanke, S. E., *in* "Sintering and Heterogeneous Catalysis" (G. C. Kuczynski, A. E. Miller, and G. A. Sargent, Eds.), *Mat. Sci. Res.,* Vol. 16, p. 223. Plenum, New York, 1984.
30. Baker, R. T. K., Prestridge, E. B., and Garten, R. L., *J. Catal.* **56,** 390 (1979); Baker, R. T. K., *Catal. Rev. Sci. Eng.* **19**(2), 161 (1979).
31. Yao, H. C., Sieg, M., and Plummer, H. K., Jr., *J. Catal.* **59,** 365 (1979).
32. Richardson, J. T., and Crump, J. G., *J. Catal.* **417** (1979).
33. Glassl, H., Kramer, R., and Hayek, K., *J. Catal.* **64,** 303 (1980).
34. Kuo, H. K., Ganesan, P., and DeAngelis, R. J., *J. Catal.* **66,** 171 (1980).
35. Straguzzi, G. I., Aduriz, H. R., and Gigola, C. E., *J. Catal.* **66,** 171 (1980).
36. Chen, J. J., and Ruckenstein, E., *J. Catal.* **69,** 254 (1981).
37. Arai, M., Ishikawa, T., Nakayama, T., and Nishiyama, Y., *J. Colloid Interface Sci.* **97,** 254 (1984).
38. Kim, K. T., and Ihm, S. K., *J. Catal.* **96,** 12 (1985).
39. Sushumna, I., and Ruckenstein, E., *J. Catal.* **94,** 239 (1985).
40. Ruckenstein, E., and Lee, S. H., *J. Catal.* **86,** 457 (1984).
41. Smith, D. J., White, D., Baird, T., and Fryer, J. R., *J. Catal.* **81,** 107 (1983).
42. Moss, R. L., *in* "Catalysis" (A Specialist Periodical Report) (C. Kemball and D. A. Dowden, Eds.), Vol. 4, p. 31. R. Soc. Chem., London, 1980.
43. Baird, T., *in* "Catalysis" (A Specialist Periodical Report) G. C. Bond and G. Webb, Eds.), Vol. 5, p. 172. R. Soc. Chem., London, 1981.
44. Burch, R. *in* "Catalysis" (A Specialist Periodical Report) (G. C. Bond and G. Webb, Eds.), Vol. 7, p. 149. R. Soc. Chem., London, 1983.
45. Dautzenberg, F. M., and Wolters, H. B. M., *J. Catal.* **51,** 26 (1978).
46. Menon, P. G., and Froment, G. F., *J. Catal.* **51,** 26 (1978).
47. Tauster, S. J., Fung, S. C., and Garten, R. L., *J. Amer. Chem. Soc.* **100,** 170 (1978).
48. References in "Metal–Support and Metal–Additive Effects in Catalysis" (B. Imelik, C. Naccache, G. Coudourier, H. Praliaud, P. Meriaudeau, P. Gallezot, G. A. Martin and J. Vedrine, Eds.). Elsevier, Amsterdam, 1982.
49. Bond, G. C., and Burch, R., *in* "Catalysis" (A Specialist Periodical Report) (G. C. Bond and G. Webb, Eds.), Vol. 6, p. 27. R. Soc. Chem., London, 1983.
50. Kunimori, K., Ikeda, Y., Soma, M., and Uchijima, T., *J. Catal.* **79,** 185 (1983).
51. Bassett, G. A., *Proc. Eur. Reg. Congr. Electron Microsc.*, Delft, **1,** 270 (1960).
52. Skofronick, J. G., and Phillips, W. B., *J. Appl. Phys.* **38,** 4791 (1967).
53. Heinemann, K., and Poppa, H., *Thin Solid Films* **33,** 237 (1976).
54. Granquist, C. G., and Buhrman, R. A., *J. Catal.* **42,** 477 (1976).
55. Granquist, C. G., and Buhrman, R. A., *J. Catal.* **46,** 238 (1977).
56. Glassl, H., Kramer, R., and Hayek, K., *J. Catal.* **63,** 167 (1980).
57. Sushumna, I., and Ruckenstein, E., *in* "Hydrogen Effects in Catalysis" (Z. Paal and P. G. Menon, Eds.). Dekker, New York, 1988.
58. Sushumna, I., and Ruckenstein, E., *J. Catal.* **108,** 77 (1987).